REGISTERED No. M. 3121

PROCEEDINGS

OF THE

INDIAN ACADEMY OF SCIENCES

VOL. XL] *SECTION A* [No. 1

JULY 1954

UNIVERSITY OF MICHIGAN
SEP 22 1954
PHYSICS LIBRARY

Price Rs. 2 or 3 Sh. *Annual Subscription Rs. 18*

PRINTED AT THE BANGALORE PRESS, BANGALORE CITY, BY C. VASUDEVA RAO,
SUPERINTENDENT AND PUBLISHED BY THE INDIAN ACADEMY OF
SCIENCES, BANGALORE.

THE STRUCTURE AND OPTICAL BEHAVIOUR OF IRIDESCENT CALCITE

By Sir C. V. Raman and A. K. Ramdas

(*Memoir No. 55, from the Raman Research Institute, Bangalore*)

Received July 16, 1954

1. Introduction

Christiaan Huygens[1] noticed that one of his specimens of iceland spar contained an inner layer exhibiting iridescence and remarked that this was parallel to one edge of the rhombohedral cleavage and equally inclined to the two others. It is now recognised that such layers arise from internal twinning and that they may be artificially produced by subjecting a crystal of calcite to suitable stresses. It is also well-known that when a distant luminous object is viewed through a rhomb of iceland spar in which such twinning is present, three images of the object are seen instead of only one; the two outer images often exhibit vivid colour, while the central or undeviated image is usually colourless. The brightness of the images, their angular separation, and the colours which they exhibit vary greatly with the direction in the crystal along which the source of light is viewed. An explanation in general terms of the origin of the two outer images and of the colour and polarisation which they display appears in Mascart's treatise.[2] Grailich[3] and later Osthoff[4] investigated the reflection and refraction of light by the twinning planes in calcite. A summary of their results is given by Pockels.[5] A noteworthy observation regarding the optical behaviour of twinned calcite is also to be found recorded in a paper by Rayleigh.[6]

Numerous specimens of transparent calcite exhibiting internal twinning were available to us in the Museum of this Institute and this induced us to undertake the study of their optical behaviour. It was immediately noticed that specimens in which twinning layers traverse the crystal simultaneously in two or even three different directions exhibit gorgeous arrays of multi-coloured images arranged in geometric patterns when a source of light is viewed through them. Plates I and II accompanying this paper reproduce photographs obtained by us of a few of the many patterns observed with the material at our disposal. A detailed examination of the case of calcite containing only a single twinning layer also revealed many facts which had apparently been overlooked by the earlier investigators. We shall refer to these in the course of the paper, the purpose of which is to present the

complete picture of the optical behaviour of iridescent calcite which has emerged from our studies.

2. GEOMETRIC THEORY

When a train of light-waves traverses a layer of calcite differing from the material on either side of it in crystallographic orientation, the waves would necessarily be reflected and refracted by the layer. Elementary considerations indicate that the angle of incidence θ_i and the angle of reflection or refraction θ_r would be related to the corresponding refractive indices μ_i and μ_r by the general formula

$$\mu_i \sin \theta_i = \mu_r \sin \theta_r. \tag{1}$$

Since the medium is birefringent, it follows that for a given angle of incidence, a wave-train of either the ordinary or the extraordinary species would, in general, give rise to *two* reflected and *two* refracted wave-trains. Other inferences from the formula are: (1) One of the refracted wave-trains emerging from the layer in each case would travel in the same direction as the incident wave-train; (2) the angles of reflection and of refraction of the ordinary wave-train would necessarily be identical; and (3) the angles of reflection as also of refraction would, in general, be greater for the extraordinary than for the ordinary wave-trains (*see* Fig. 1 and Fig. 2 below in which these results are embodied).

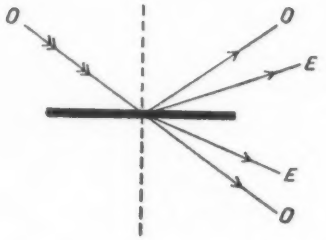

FIG. 1.

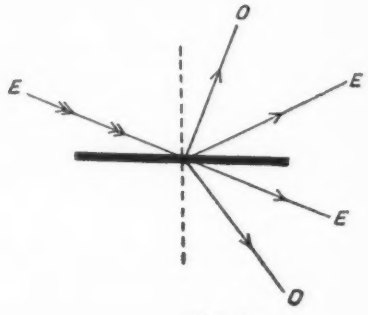

FIG. 2.

Reflection and Refraction by a Twinning Layer.

When a distant source of light is viewed through the opposing pair of faces of a cleavage rhomb of iceland spar, we observe only a single image of the source, though the wave-trains divide into the ordinary and extraordinary species and follow different paths within the crystal. It is readily seen from Figs. 1 and 2 that the same situation would subsist even when a twinning layer is present and is traversed by these waves. In such a case, however, the ordinary wave-train which emerges as an extraordinary one

and the extraordinary wave-train which emerges as an ordinary one after passage through the layer, would both give rise to additional images, deviated respectively to one side and the other of the principal image. The magnitude of their angular deviations may be deduced at once from the general formula and is the smaller, the more nearly the direction of observation through the crystal approaches the optic axis. It is important to remark that while the central or undeviated image would appear in the same direction for all wavelengths, such would not be the case for the deviated images. The dispersion of the refractive indices in calcite is very different for the ordinary and the extraordinary waves. Hence, the two lateral images would appear drawn out into spectra, and it may be remarked that such dispersion would be large when the wave-train under consideration emerges nearly parallel to the twinning layer.

The general formula indicates other results of interest. If μ_i be the ordinary and μ_r the extraordinary index, θ_r would be real only if $\theta_i \leqslant \sin^{-1}\mu_r/\mu_i$. At the upper limit indicated, the reflected and refracted extraordinary waves would emerge parallel to the twinning layer, while for greater incidences they are non-existent. Likewise, when μ_i is the extraordinary and μ_r the ordinary index, $\theta_r \leqslant \sin^{-1}\mu_i/\mu_r$: the limiting value is reached when the incident waves graze the twinning layer. In both cases, the limiting angle may be written as $\sin^{-1}\mu_e/\mu_o$ where μ_o is the ordinary index and μ_e is the extraordinary index for the direction of propagation parallel to the twinning layer in the plane of incidence. Thus, if light be incident on a twinning layer simultaneously in all directions, a boundary line may be drawn in the field separating the directions of incidence of the ordinary wave-trains which give rise to extraordinary reflections and refractions and of those which do not. Likewise, the optical fields traversed by the reflected and refracted wave-trains are, each of them, divided by a boundary line on the two sides of which ordinary wave-trains resulting from incident extraordinary ones respectively appear and do not appear.

It is evident from the foregoing remarks that we cannot always expect to be able to observe the deviated images on both sides of the principal image when a distant light source is viewed through a calcite rhomb. As the angle of incidence on the twinning layer approaches and ultimately exceeds the limiting value, the extra-ordinary refraction resulting therefrom would emerge parallel to the twinning layer and ultimately disappear.

3. Intensity Considerations

A factor which greatly influences the observed phenomena is the azimuth of the plane of incidence of the light on the twinning layer. It has

already been remarked that the layer is parallel to one of the edges of the rhombohedral cleavage and equally inclined to the two others. It follows that a plane through the edge first mentioned which is perpendicular to the lamina would contain the optic axis of the calcite crystal and the optic axis of the twinning layer as well. The plane under reference would thus be a plane of symmetry for the entire crystal including the twinning layer. As in the case of potassium chlorate recently discussed in these *Proceedings*,[7] it can be shown from elementary considerations that when the plane of incidence of the light coincides with this symmetry plane, reflections and refractions would disappear and the incident light-waves would emerge from the twinning layer with their direction of propagation as well as their intensity unaltered.

The foregoing conclusion is readily tested by viewing a distant source of light through the calcite rhomb held in front of the eye of the observer in such manner that the twinning layer is vertical while the plane of observation is horizontal; the source should be viewed through the faces of the rhomb which are bounded by edges of which none is parallel to the twinning layer. Only the undeviated image of the source can then be seen. But if the crystal is slightly tilted about a horizontal axis so that the plane of incidence of the light ceases to be horizontal, the deviated images make their appearance, and rapidly gain in intensity as the plane of incidence is turned away from the horizontal in either sense.

An interesting modification of this experiment is to view an extended area of illumination through the faces of the rhomb held in the manner indicated above and to rotate the rhomb about a vertical axis so that the plane of the twinning layer remains vertical but alters its orientation with respect to the direction of observation. A division of the field of observation into two parts differing in their intensity of illumination then comes into view. A dark and sharply defined boundary is seen to separate the two parts of the field except where it is cut by the horizontal symmetry plane. This dividing boundary becomes more and more conspicuously observable as we move away from the symmetry plane in either direction. Interposing a polaroid in front of the rhomb, it is found that the division of the field into two parts and the dark boundary separating them are most conspicuous when the vibration direction of the polaroid is vertical, but disappear when the same is horizontal. It is thereby made evident that the boundary is the one indicated by the geometric theory as the limit of the angle of incidence of the ordinary waves on the twinning layer beyond which the extraordinary reflections and refractions disappear. That the boundary vanishes in the symmetry plane and becomes more conspicuous as we move away from it

is to be expected in the circumstances. The boundary is sharply defined evidently as a consequence of the weakening of the ordinary transmission by reason of the extraordinary reflections and refractions reaching their maximum intensity just prior to their disappearance at the limiting incidence.

A slight modification of the arrangements described above enables us to observe the boundaries at which the reflections and refractions of the extraordinary waves as ordinary waves terminate. For this purpose, the illuminated screen is held to one side so that the light reflected or refracted by the twinning layer comes into the field of view. The boundary is seen then as an arc of light bordered by coloured fringes and separating a bright from a dark part of the field of view. The bright arc is however interrupted at the symmetry plane, and gains in intensity as we move away from that plane in either direction. By inserting a polaroid before and after the calcite rhomb respectively, it is readily demonstrated that the luminous arc has its origin in the trains of extraordinary waves which are transformed to ordinary ones by reflection or by refraction. The sharpness and brilliancy of the boundary are to be expected alike on geometrical and physical considerations.

4. Interference Phenomena

As has been already remarked, the deviated images of a distant light source seen through the twinning layer are spread out into spectra by reason of the difference in the dispersive powers of calcite for the ordinary and extraordinary waves. Using a narrow slit as the source of light, these spectra can be readily observed and are found to be chanelled by interference bands crossing them. The position and number of the interferences vary with the specimen under observation and thus evidently depend on the thickness of the twinning layer in each particular case. Careful examination reveals that we have two sets of interferences simultaneously present in the spectra, one of which is on a finer scale than the other. The explanation of these effects is not far to seek. Returning to the Text-Figs. 1 and 2 above, it will be evident that in the passage of the incident waves through the twinning layer, the birefringence of the latter would come into play. Hence, each of the wave-trains reflected or refracted by the layer would itself be the resultant of the wave-trains of the two different species possible within the layer, the optical paths of which would be different. Interferences of the same nature as those exhibited by crystalline plates in polarised light would therefore arise and would manifest themselves in the spectral character of the reflected and refracted wave-trains. Effects of the same nature as the ordinary interferences of thin plates would also simultaneously appear. The colours

observed with extended light sources are a consequence of both species of interference.

Interference phenomena are also strikingly manifested at and near the boundaries of transmission, reflection and refraction considered in the preceding section. They take the form of alternate dark and bright bands of varying sharpness and intensity fringing the boundaries referred to. There again, we observe two species of interference, one of which is on a finer scale than the other. These boundary effects are best studied using a diffusing screen illuminated by a monochromatic source, though indeed they can be also observed with white light.

5. EFFECTS OBSERVED WITH MULTIPLY TWINNED CALCITE

We now turn to a consideration of the phenomena, typical examples of which are reproduced as Figs. 1, 2, 3 and 4 in Plates I and II accompanying the paper. The photographs reproduced were obtained using a small aperture backed by a tungsten filament lamp as the source of light. A photographic camera placed about three metres away was focussed on the source, the calcite rhomb being placed immediately in front of the lens. Panchromatic plates were employed for recording the patterns. The brilliant colour effects actually observed are, of course, not reproduced.

Figure 1 shows the three images observed with a calcite rhomb having a single twinning layer. In addition to the bright images, we observe a system of bright streaks, as also some diffuse light surrounding the images. The surfaces of the cleavage rhombs had not been specially polished and their unevenness was no doubt in part responsible for some of the unwanted effects. Nevertheless, our studies with numerous specimens left little doubt that the long bright streaks appearing in the photographs and also seen visually had their origin within the calcite rhombs. It appears reasonable to attribute them to a lack of perfect smoothness of the twinning layers within the crystal.

Another remark may usefully be made with regard to Fig. 1 in the Plate. This was recorded through the faces of the calcite rhomb which had two of their edges parallel to the twinning layer. In these circumstances, the plane of incidence of the light on the twinning layer was, in general, far removed from the symmetry plane. By turning the crystal about one edge, the images could be made to approach towards or recede from each other. Simultaneously, there were large changes in the colour and intensity of the images. At particular settings which were nearly but not quite coincident, the two outer images vanished but on further rotation they reappeared in positions closer still to the principal image. The observations indicated

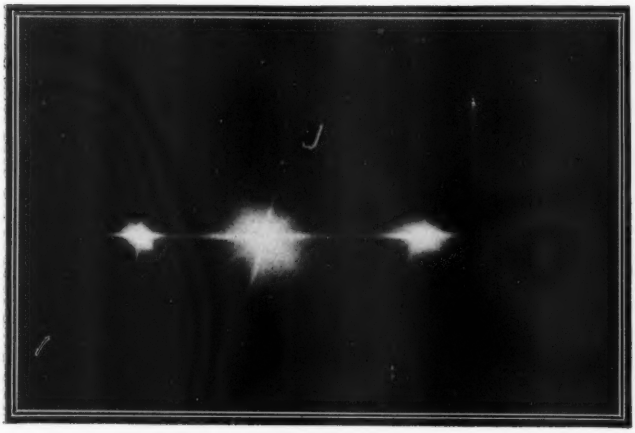

FIG. 1

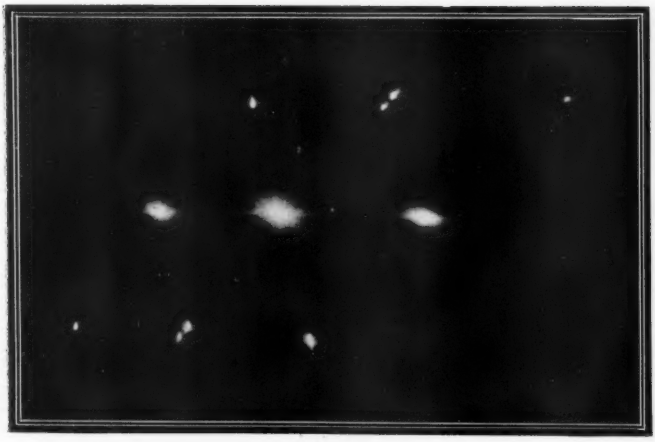

FIG. 2

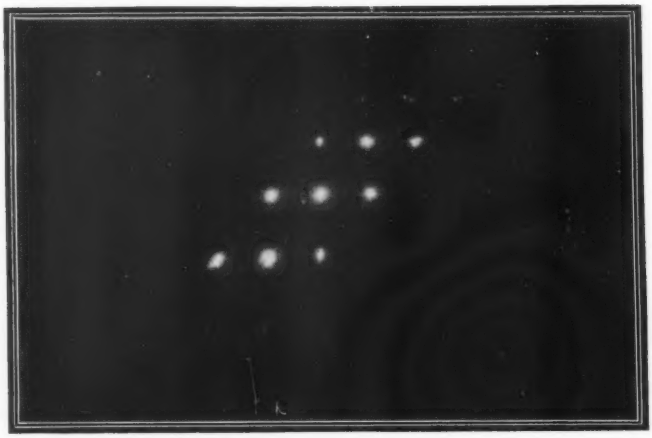

FIG. 3

FIG. 4

that for the settings at which the images disappeared, the plane of incidence was nearly coincident with the symmetry plane.

Figure 2 in Plate I shows the pattern of a type frequently observed by us and which arises from the simultaneous action of twinning layers parallel to two of the edges of the rhombohedral cleavage. A noteworthy feature in the photograph is that the middle spot in the outer rows has split into two components. These were found to be polarised in perpendicular directions. Figs. 3 and 4 represent more complicated cases. It is to be noted that the spots appear in groups of threes, with the middle one in each row distinctly separated into two components. All the patterns exhibited special features of polarisation analagous to those observed in the simple case of a single twinning layer.

6. Summary

Arrays of multi-coloured images of a distant light-source arranged in geometric patterns are exhibited by calcite rhombs traversed by twinning layers in several directions simultaneously. The paper reproduces four photographs of such patterns and also discusses the theory of the reflection and refraction of light by twinning layers in calcite. The large difference between the ordinary and extra-ordinary dispersive powers results in a linear source observed through such a layer appearing drawn out into spectra chanelled by interferences. Interference bands also fringe the sharply defined boundaries seen separating the different parts of the optical field of reflection and refraction.

7. References

1. Christiaan Huygens .. *Treatise on Light*, English Translation by Silvanus Thompson, University of Chicago Press, 98.
2. Mascart .. *Traite' D'Optique*, **2**,
3. Grailich .. *Pogg. Ann.*, 1856, **98**, 205.
4. Osthoff .. *N. Jahrb. f. Miner. Beil-Bd.* **20**,
5. Pockels .. *Lehrbuch Der Kristalloptik*, 203.
6. Rayleigh .. *Scientific Papers*, **3**, 212
7. Raman and Krishnamurti .. *Proc. Ind. Acad. Sci.*, 1953, **38 A**, 263.

ON THE DISTRIBUTION OF THERMAL NEUTRONS FROM A FAST NEUTRON SOURCE PLACED AT THE INTERFACE OF TWO MEDIA

By R. Ramanna* and S. B. D. Iyengar

(*Tata Institute of Fundamental Research, Bombay*)

Received April 23, 1954

(Communicated by Dr. H. J. Bhabha, F.R.S., F.A.SC.)

1. Introductory

The object of the investigation is to determine the effect of a paraffin reflector on the spatial distribution of thermal neutrons due to a point source of fast neutrons kept at the surface of a graphite moderator. If the effect of the reflector is to reduce the leakage of neutrons from the sides of the graphite without appreciably reducing the total flux due to its own absorption, it may be possible to avoid the use of expensive graphite for reflector and use paraffin or water instead.

In order to determine the effect of the reflector, the thermal neutron density in a graphite medium due to a point fast neutron source placed on its surface and covered by (1) a paraffin reflector and (2) a graphite reflector was measured. An expression was obtained for the thermal neutron flux in a medium due to a point fast neutron source on the interface between it and another medium, by means of the two group theory. The experimental results were compared with the theoretical distribution. The results were also compared with a theoretical distribution for a uniform plane fast neutron source, by integrating the results for the point source at various points. The agreement between theory and experiment is discussed.

2. Theory

Let A be a cylindrical block of moderator of radius R and length L_A and B a cylindrical block of reflector of same radius and length L_B. At the centre of the interface is kept a point source of fast neutrons of strength S_0. If we suppose that the neutrons in the medium A are divided into 2 groups, one fast and one thermal, then we can write for the fast group flux,

$$D_{1A}\nabla^2\phi_{1A} - \Sigma_{1A}\phi_{1A} = 0, \qquad (1)$$

* Reactor group, Atomic Energy Commission.

where the subscript 1 refers to the fast group,

ϕ_{1A} is the fast group flux,

Σ_{1A} the slowing down cross-section, and

D_{1A} the fast diffusion coefficient.

For the thermal group flux,

$$D_{2A} \nabla^2 \phi_{2A} - \Sigma_{2A} \phi_{2A} + \Sigma_{1A} \phi_{1A} = 0 \tag{2}$$

where the subscript 2 refers to the thermal group,

ϕ_{2A} is the thermal group flux,

Σ_{2A} is the macroscopic absorption cross-section

and

D_{2A} the thermal diffusion coefficient.

Similarly, in the medium B,

$$D_{1B} \nabla^2 \phi_{1B} - \Sigma_{1B} \phi_{1B} = 0, \tag{3}$$

$$D_{2B} \nabla^2 \phi_{2B} - \Sigma_{2B} \phi_{2B} + \Sigma_{1B} \phi_{1B} \tag{4}$$

where D_{1B}, D_{2B}, Σ_{1B} and Σ_{2B} are the corresponding constants for the medium B. If we write the solution of equation (1) as Z_1, we can write a solution of equation (2) as $Z_2 + S_A Z_1$ where Z_2 is a solution of

$$D_{2A} \nabla^2 \phi_{2A} - \Sigma_{2A} \phi_{2A} = 0.$$

Similarly we can write the solutions of (3) and (4) as

$$Z_2 \text{ and } Z_4 + S_B Z_3.$$

By substitution we have

$$S_A = \frac{\Sigma_{1A}}{D_{2A}} \frac{1}{p_{2A}^2 - p_{1A}^2}, \tag{5}$$

$$S_B = \frac{\Sigma_{1B}}{D_{2B}} \frac{1}{p_{2B}^2 - p_{1B}^2}, \tag{6}$$

where

$$p_{1A} = \sqrt{\frac{\Sigma_{1A}}{D_{1A}}}, \; p_{2A} = \sqrt{\frac{\Sigma_{2A}}{D_{2A}}}, \; p_{1B} = \sqrt{\frac{\Sigma_{1B}}{D_{1B}}}, \; p_{2B} = \sqrt{\frac{\Sigma_{2B}}{D_{2B}}} \tag{7}$$

At first we shall suppose that the source is not a point source but a plane source distributed over the interface, the strength of the source being a function only of the distance from the centre. Let $S(r)$ be the strength per unit

area of the source at distance r from the centre. The equations are all essentially of the type (1), and are solved by separation of variables in cylin-

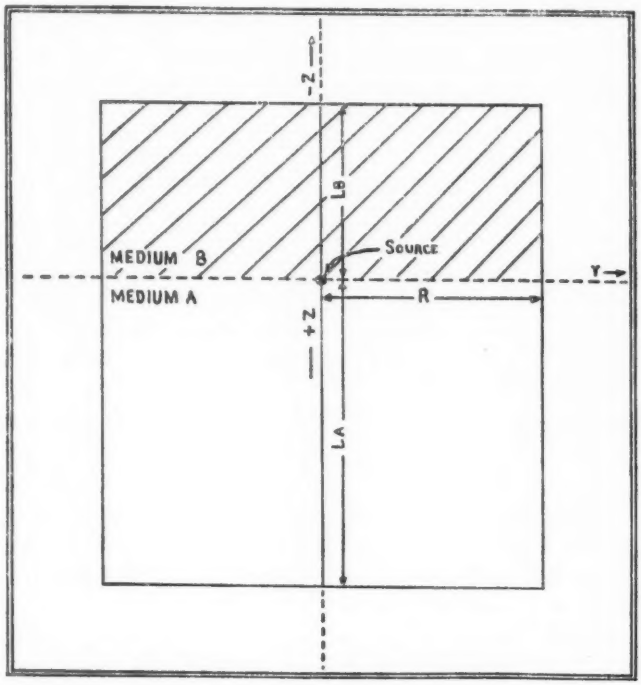

FIG. 1

drical co-ordinates taken as shown in Fig. 1. Due to symmetry about the z-axis, there are only two variables. We obtain

$$\phi_{1A} = [A_{1k} e^{\alpha z} + A'_{1k} e^{-\alpha z}] [C_{1k} J_0 (kr) + C'_{1k} Y_0 (kr)]$$

$$\phi_{2A} = [A_{2k} e^{\gamma z} + A'_{2k} e^{-\gamma z}] [C_{2k} J_0 (kr) + C'_{2k} Y_0 (kr)] + S_A \phi_{1A}$$

and similar expressions for ϕ_{1B} and ϕ_{2B}, where

$$\alpha = \sqrt{k^2 + p_{1A}{}^2},\ \beta = \sqrt{k^2 + p_{1B}{}^2},\ \gamma = \sqrt{k^2 + p_{2A}{}^2},\ \delta = \sqrt{k^2 + p_{2B}{}^2} \quad (8)$$

the solutions being summed over all possible values of the separation constant k. Our solutions must satisfy the following boundary conditions:

(1) The ϕ's should be finite at all points. The coefficients of the $Y_0(kr)$ terms should therefore be zero.

$$C'_{1k} = C'_{2k} = 0, \text{ etc.}$$

(2) At $z = L_A$, $\phi_{1A} = 0$, $\phi_{2A} = 0$, for all values of r, *i.e.*,

$$A_{1k} = -A'_{1k}\, e^{-2\alpha L_A},\quad A_{2k} = -A'_{2k}\, e^{-2\gamma L_A}$$

At $z = -L_B$, $\phi_{1B} = 0$, $\phi_{2B} = 0$ for all values of r, *i.e.*,

$$B'_{1k} = -B_{1k}\, e^{-2\beta L_B},\quad B'_{2k} = -B_{2k}\, e^{-2\delta L_B}$$

(3) At $r = R$, $\phi_{1A} = \phi_{2A} = \phi_{1B} = \phi_{2B} = 0$, for all values of z, *i.e.*,

$$J_0(kR) = 0.$$

k can only take values $k_1, k_2, \ldots k_n, \ldots\ldots$ etc.

where these are the solutions of above equation for k. Making use of the above relations our solutions can be written as

$$\phi_{1A} = \sum_{n=1}^{\infty} A_{1n} \left[e^{-\alpha_n z} - e^{\alpha_n (z - 2L_A)}\right] J_0(k_n r), \tag{9 a}$$

$$\phi_{2A} = \sum_{n=1}^{\infty} A_{2n} \left[e^{-\gamma_n z} - e^{\gamma_n (z - 2L_A)}\right] J_0(k_n r) + S_A \phi_{1A}, \tag{9 b}$$

$$\phi_{1B} = \sum_{n=1}^{\infty} B_{1n} \left[e^{\beta_n z} - e^{-\beta_n (z + 2L_B)}\right] J_0(k_n r), \tag{9 c}$$

$$\phi_{2B} = \sum_{n=1}^{\infty} B_{2n} \left[e^{\delta_n z} - e^{-\delta_n (z + 2L_B)}\right] J_0(k_n r) + S_B \phi_{1B}. \tag{9 d}$$

(4) At the interface, *i.e.*, at $z = 0$,

$\phi_{1A} = \phi_{1B}$, and $\phi_{2A} = \phi_{2B}$ for all values of r. Hence

$$\sum_{n=1}^{\infty} A_{1n} (1 - e^{-2\alpha_n L_A}) J_0(k_n r) = \sum_{n=1}^{\infty} B_{1n} (1 - e^{-2\beta_n L_B}) J_0(k_n r),$$

$$\sum_{n=1}^{\infty} A_{2n} (1 - e^{-2\gamma_n L_A}) J_0(k_n r) + S_A \sum_{n=1}^{\infty} A_{1n} (1 - e^{-2\alpha_n L_A}) J_0(k_n r)$$

$$= \sum_{n=1}^{\infty} B_{2n} (1 - e^{-2\delta_n L_B}) J_0(k_n r) + S_B \sum_{n=1}^{\infty} B_{1n} (1 - e^{-2\beta_n L_B}) J_0(k_n r).$$

Multiplying the first relation on both sides by $r\, J_0(k_m r)$ and integrating with respect to r between 0 and R, we get

$$\sum_{n=1}^{\infty} A_{1n}(1 - e^{-2\alpha_n L_A}) \int_0^R r\, J_0(k_m r) J_0(k_n r)\, dr$$

$$= \sum_{n=1}^{\infty} B_{1n}(1 - e^{-2\beta_n L_B}) \int_0^R r\, J_0(k_m r)\, J_0(k_n r)\, dr,$$

which simplifies to

$$A_{1m}(1 - e^{-2\alpha_m L_A}) = B_{1m}(1 - e^{-2\beta_m L_B}) \tag{10}$$

Similarly from the other relation

$$A_{2m}(1 - e^{-2\gamma_m L_A}) + S_A A_{1m}(1 - e^{-2\alpha_m L_A})$$

$$= B_{2m}(1 - e^{-2\delta_m L_B}) + S_B B_{1m}(1 - e^{-2\beta_m L_B}) \tag{11}$$

(5) At the interface, *i.e.*, at $z = 0$,

$(J_{1A})_z - (J_{1B})_z = S(r)$, and $(J_{2A})_z - (J_{2B})_z = 0$ for all values of r, $(J_{1A})_z$ being the z-component of the current density J_{1A}, etc.

$$(J_{1A})_z = -D_{1A} \frac{\partial \phi_{1A}}{\partial z}, \text{ etc.}$$

From (9), we then have

$$(J_{1A})_z = D_{1A} \sum_{n=1}^{\infty} \alpha_n A_{1n} [e^{-\alpha_n z} + e^{\alpha_n (z - 2L_A)}] J_0(k_n r).$$

We obtain similar expressions for $(J_{2A})_z$, $(J_{1B})_z$ and $(J_{2B})_z$.
We then otain

$$D_{1A} \sum_{n=1}^{\infty} \alpha_n A_{1n}(1 + e^{-2\alpha_n L_A}) J_0(k_n r) + D_{1B} \sum_{n=1}^{\infty} \beta_n B_{1n}(1 + e^{-2\beta_n L_B}) J_0(k_n r)$$

$$= S(r).$$

$$D_{2A} \sum_{n=1}^{\infty} \gamma_n A_{2n}(1 + e^{-2\gamma_n L_A}) J_0(k_n r) + D_{2A} S_A \sum_{n=1}^{\infty} A_{1n}(1 + e^{-2\alpha_n L_A}) J_0(k_n r)$$

$$= -D_{2B} \sum_{n=1}^{\infty} \delta_n B_{2n}(1 + e^{-2\delta_n L_B}) J_0(k_n r) - D_{2B} S_B \sum_{n=1}^{\infty} \beta_n B_{1n}(1 + e^{-\beta_n L_B}) J_0(k_n r)$$

Multiplying both sides by $r\, J_0(k_m r)$ and integrating with respect to r between 0 and R and simplifying, we obtain

$$D_{1A} \alpha_m A_{1m}(1 + e^{-2\alpha_m L_A}) + D_{1B} \beta_m B_{1m}(1 + e^{-2\beta_m L_B})$$

$$= \frac{\int_0^R S(r)\, r\, J_0(k_m r)\, dr}{\frac{1}{2} k_m^2 R^2 [J_1(k_m R)]^2} \tag{12}$$

$$D_{2A}\gamma_m A_{2m}(1+e^{-2\gamma_m L_A}) + D_{2A} S_A \alpha_m A_{1m}(1+e^{-2\alpha_m L_A}) = -D_{2B}\delta_m B_{2m}(1+e^{-2\delta_m L_B}) - D_{2B} S_B \beta_m B_{1m}(1+e^{-2\beta_m L_B}) \quad (13)$$

Solving (10), (11), (12) and (13) for the constants and substituting in (9) we get

$$\phi_{1A} = \sum_{n=1}^{\infty} \frac{C_n}{1-e^{-2\alpha_n L_A}} \left[e^{-\alpha_n z} - e^{\alpha_n (z-2L_A)}\right] J_0(k_n r) \quad (14\,a)$$

$$\phi_{1B} = \sum_{n=1}^{\infty} \frac{C_n}{1-e^{-2\beta_n L_B}} \left[e^{\beta_n z} - e^{-\beta_n (z+2L_B)}\right] J_0(k_n r) \quad (14\,b)$$

$$\phi_{2A} = \sum_{n=1}^{\infty} C_n \left[A_n (e^{-\gamma_n z} - e^{\gamma_n (z-2L_A)}) + \frac{S_A (e^{-\alpha_n z} - e^{\alpha_n (z-2L_A)})}{1-e^{-2\alpha_n L_A}}\right] J_0(k_n r) \quad (14\,c)$$

$$\phi_{2B} = \sum_{n=1}^{\infty} C_n \left[B_n (e^{\delta_n z} - e^{-\delta_n (z+2L_B)}) + \frac{S_B (e^{\beta_n z} - e^{-\beta_n (z+2L_B)})}{1+e^{-2\beta_n L_B}}\right] J_0(k_n r) \quad (14\,d)$$

where

$$C_n = \frac{2\int_0^R S(r)\, r\, J_0(k_n r)\, dr}{[D_{1A}\alpha_n \coth(\alpha_n L_A) + D_{1B}\beta_n \coth(\beta_n L_B)] k_n^2 R^2 [J_1(k_n R)]^2} \quad (15)$$

$$A_n = \frac{S_B D_{2B}[\delta_n \coth(S_n L_B) - \beta_n \coth(\beta_n L_B)] - S_A [D_{2A}\alpha_n \coth \alpha_n L_A + D_{2B}\delta_n \coth(\delta_n L_B)]}{(1-e^{-2\gamma_n L_A})[D_{2A}\gamma_n \coth(\gamma_n L_A) + D_{2B}\delta_n \coth(\delta_n L_B)} \quad (16)$$

With a similar expression for B_n.

To apply these results to the case of a point source, $S(r)$ must be of such a form that

$$S(r) = 0 \text{ when } r \neq 0$$

and the total number of neutrons emitted by the interface should be equal to S_0

$$\int_0^R S(r) \cdot 2\pi r dr = S_0$$

If $S(r) = \frac{S_0 \delta(r)}{\pi r}$, $\delta(r)$ being the Dirac Delta-function, these conditions are satisfied. Substituting this expression for $S(r)$ in equation (15), we obtain

$$C_n = \frac{S_0}{\pi [D_{1A} \alpha_n \coth(\alpha_n L_A) + D_{1B} \beta_n \coth(\beta_n L_B)] k_n^2 R^2 [J_1(k_n R)]^2} \quad (17)$$

With this value of C_n equations (14) give the final solution.

The problem was also solved for a uniform plane source distribution on the interface. There is now only one co-ordinate z and the cylinders become of infinite radius. Let S be the strength of source per unit area.

The solutions are:

$$\phi_{1A} = \frac{C}{1 - e^{-2p_{1A}L_A}} [e^{-p_{1A}z} - e^{p_{1A}(z-2L_A)}] \quad (18)$$

$$\phi_{2A} = C \left[A (e^{-p_{2A}z} - e^{p_{2A}(z-2L_A)}) + \frac{S_A (e^{-p_{1A}z} - e^{p_{1A}(z-2L_A)})}{1 - e^{-2p_{1A}L_A}} \right] \quad (19)$$

where

$$C = \frac{S}{D_{1A} p_{1A} \coth(p_{1A} L_A) + D_{1B} p_{1B} \coth(p_{1B} L_B)}$$

$$A = \frac{(S_B - S_A) D_{2B} p_{2B} \coth(p_{2A} L_A) - [D_{2A} p_{1A} \coth(p_{1A} L_A) + D_{2B} p_{1B} \coth(p_{1B} L_B)]}{(1 - e^{-2p_{2A}L_A}) [D_{2A} p_{2A} \coth(p_{2A} L_A) + D_{2B} p_{2B} \coth(p_{2B} L_B)]}$$

EXPERIMENT

The experimental arrangement for the measurement of the thermal neutron distributions is shown in Fig. 2. It consisted of a large graphite

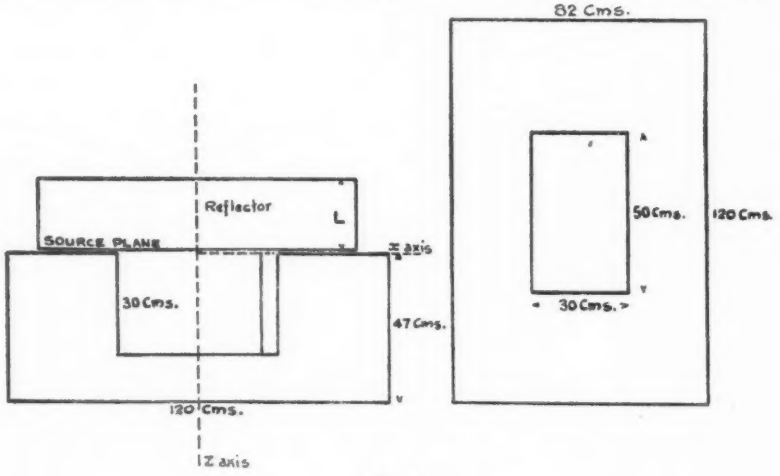

FIG. 2

block 120 cm. wide, 80 cm. long and 47 cm. deep with a rectangular cavity of depth 30 cm. from one surface for introducing the detectors. The space was then refilled with graphite bricks and covered by a paraffin or graphite reflector as the case may be. The neutron densities were measured by means of the activation of Mn-Ni foils previously calibrated for relative efficiency. The foils were placed one below the other inside slits cut in a graphite brick and then placed in the required position inside the rectangular space. A Ra-Be neutron source of 50 mc. strength was placed in various positions along the reflector-graphite interface and the activation of the foils for each position of the source was measured. The counting assembly consisted of

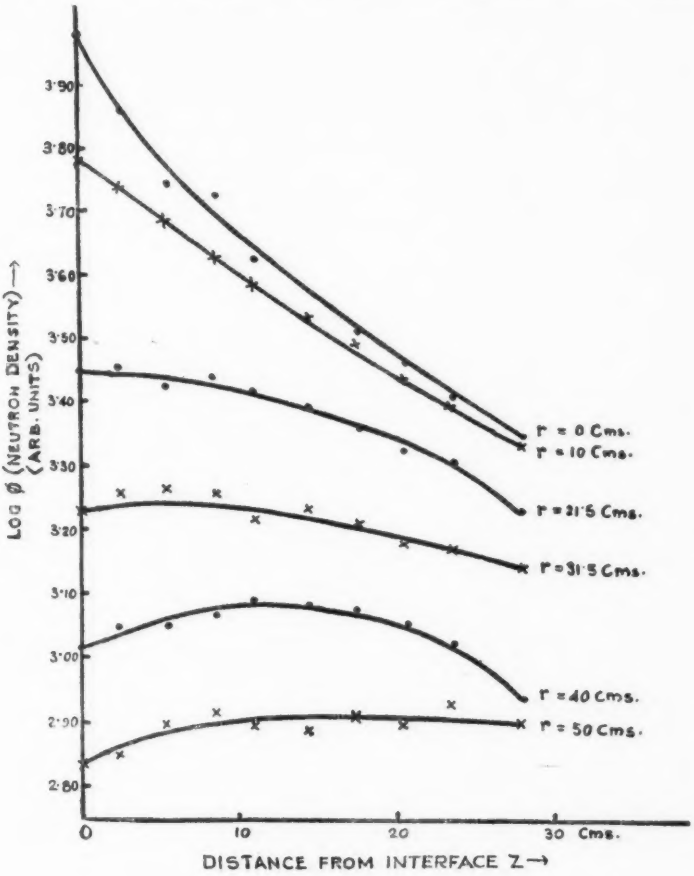

FIG. 3

a pair of geiger counters in parallel shielded for cosmic rays and a conventional counting equipment.

It will be seen that the geometry of the experiment does not exactly coincide with the geometry assumed for deriving the theoretical expression. The graphite and paraffin blocks are not cylindrical, the source is not always at the geometrical centre of the interface and the detectors are also not along the central axis. But due to the large size of blocks, the exact geometry ceases to be of importance. The source and detectors though asymmetrically placed are not far from the central axis, there being at least 35 cm. of graphite surrounding them on the thinnest side. So the theoretical expression may be applied to explain the results of the experiment.

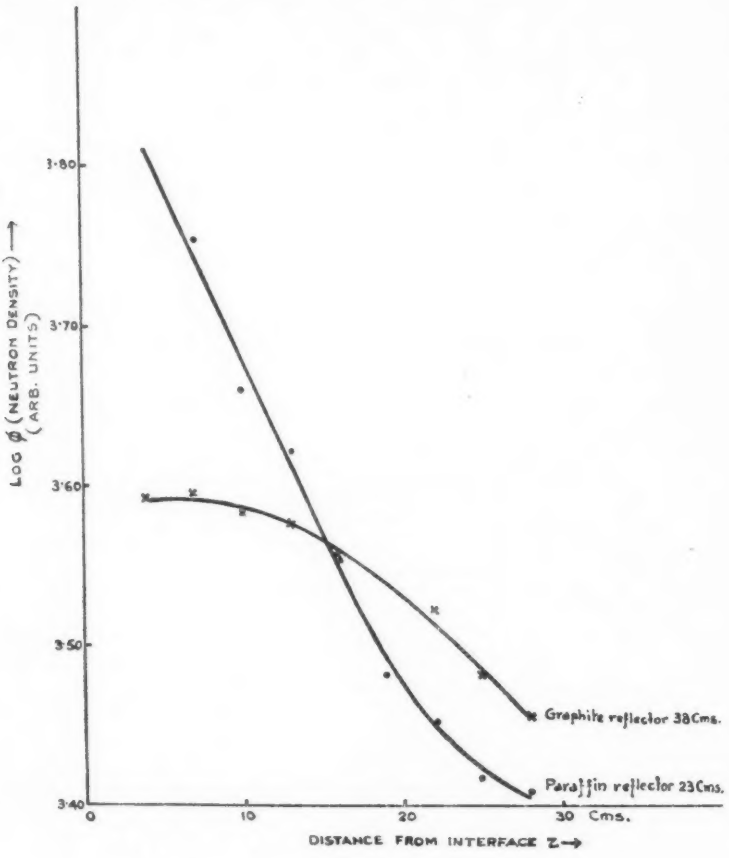

FIG. 4

Fig. 3 shows the variation of Log. (thermal neutron flux) with z, for various values of r.

The experiment was also performed with a graphite reflector but for only one position of source with $r = 0$. The Log. (thermal neutron flux) is plotted against z, for $r = 0$, for both graphite and paraffin reflector in Fig. 4. The paraffin value is higher than the graphite value for small values of z, but at about $z = 15{\cdot}5$ cm. it becomes equal and then becomes less than the graphite value.

In order to determine the flux distribution for a plane source, the surface around the point $r = 0$, was divided into concentric rings, of width

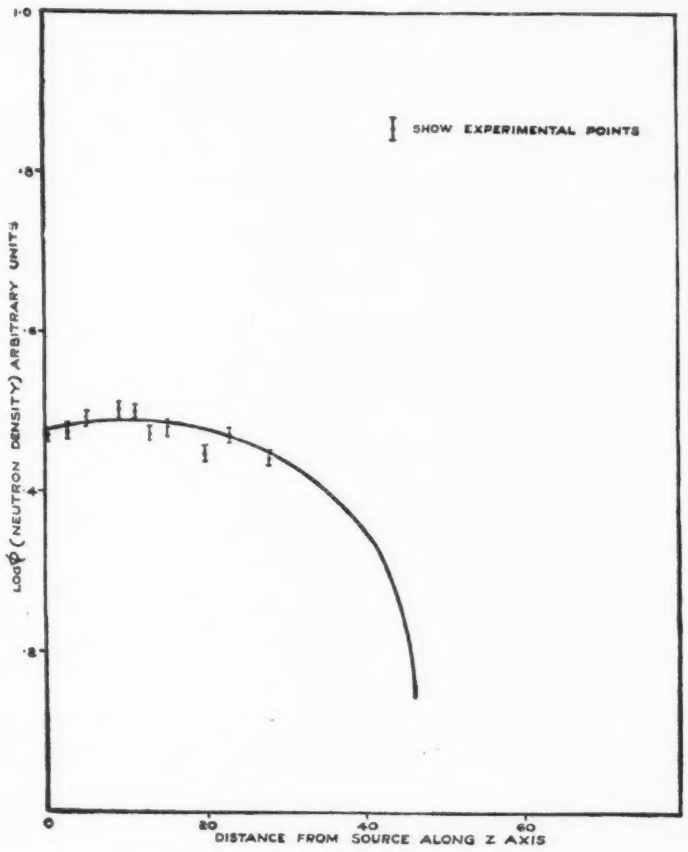

FIG. 5

10 cm. corresponding to the various values of r, and the contributions to any point along the z-axis from these various rings were integrated and the flux due to a plane source disc of 55 cm. radius was obtained. Fig. 5 shows the Log. (thermal neutron density) points so obtained and also the theoretical curves obtained from expression (19) for paraffin. The agreement, it will be seen, is quite good.

Values of ϕ_{2A} the thermal neutron density for various values of r and z were calculated from expression (14 c). The constants for paraffin and graphite used for the purpose are shown in the appendix.

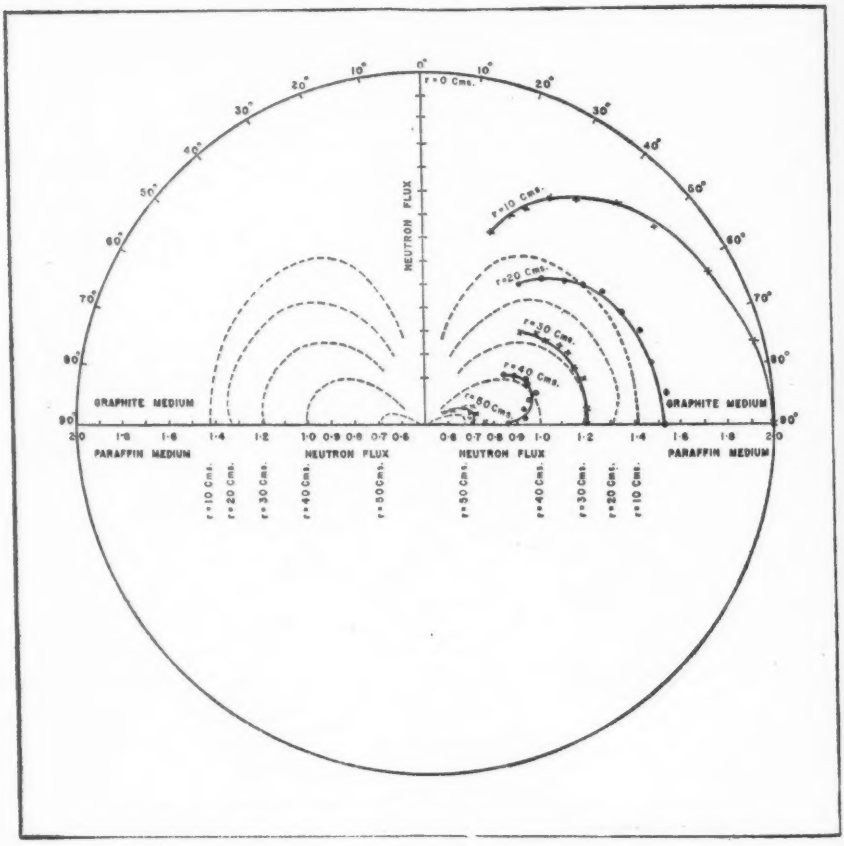

FIG. 6

Fig. 6 shows a polar diagram of Log. ϕ_{2A} plotted against θ, the angle between the line joining the point to the source and the z-axis, for points lying along straight lines parallel to the z-axis at various distances r from it. The diagram shows theoretical curves for $r = 0$, 10, 20, 30, 40 and 50 cm., with experimental points also indicated. It can be noted that for $r = 0$ the curve is just a straight line. It will be seen that the agreement between theory and experiment is good for large values of z and r but poor for small values. This may be explained as due to the fact that the assumptions on which the theoretical result is derived, such as that simple diffusion theory applies

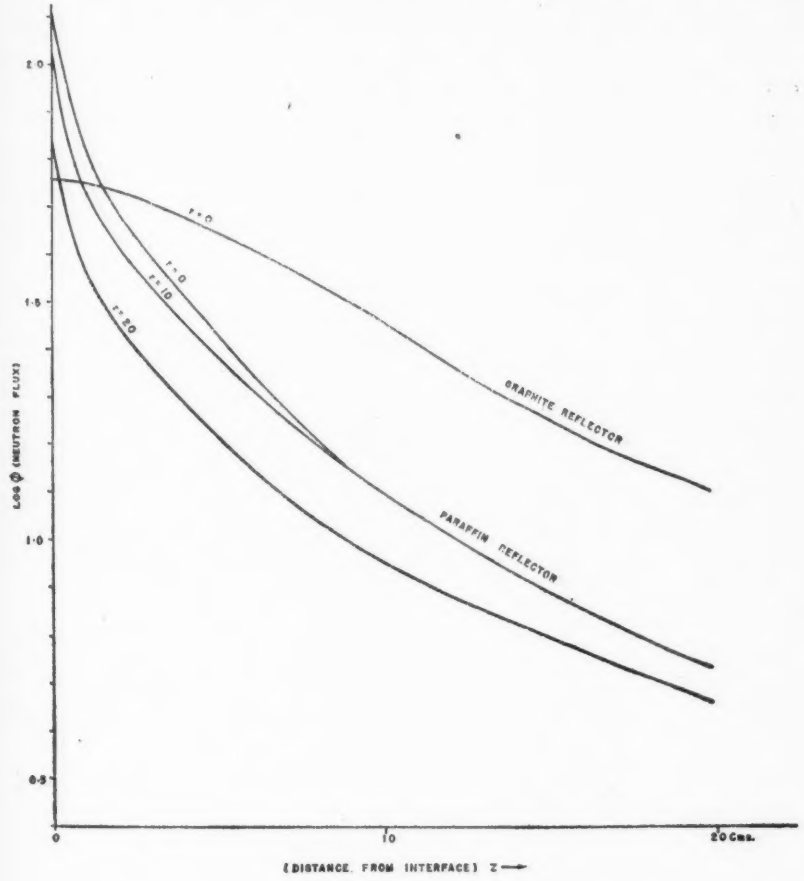

FIG. 7

throughout the region and that the source is a point source, become untenable at small distances from source.

A calculation from (14 *c*) of the flux for the paraffin and the graphite reflector for $r = 0$ showed that the graphite values are always much higher than the paraffin values. This led us to consider that the graphite used may not have been quite pure. The values of the constants mentioned in the Appendix, are for graphite with impurity less than 2 parts per million, the impurity being wholly due to boron content. If greater contamination of boron is considered, the other constants remain practically unchanged but the value of p_2 increases. Calculations were made for various values of p_2 and Fig. 7 shows the theoretical curves for a paraffin reflector for three values of r and for a graphite reflector for $r = 0$, for an arbitrary value of $p_2 = 1$. It is seen that these curves agree qualitatively with those of the experimental curves given in Fig. 4 only for this very high value of p_2, the paraffin value being more than that of graphite for lower value of z and less than the graphite for higher value of z. A closer fit to the experiment was not attempted as the exact value of p_2 to fit the experimental results was not of any particular importance.

It appears that on the two group theory for pure graphite the use of the paraffin instead of the graphite reflector reduces substantially the thermal neutron flux, the intensity at $z = 0$ for the paraffin reflector being only 0·34 times the value for the graphite reflector. For larger values of z this ratio continues to have almost the same value.

The experimental part of this work was done at the Centre d'Études Nucléaires, Saclay, Paris. One of us (R.R.) has pleasure in thanking the Commissariat a l'Energie Atomique, France, for providing the facilities to perform the experiment and also in thanking M. Martelly for many useful discussions. Our thanks are also due to Dr. H. J. Bhabha for his encouragement during the course of this work.

APPENDIX

Constant	Graphite	Paraffin
Slowing down Cross-Section	0·00302	0·0505
Fast Diffusion Coefficient	1·057	1·515
Macroscopic abs. Cross-Section	0·00036	0·017
Diffusion Coefficient (thermal)	0·903	0·142
$p_1 = \frac{\Sigma_1}{D_1}$ ..	0·0535	0·175
$p_2 = \frac{\Sigma_2}{D_2}$	0·01997 (†)	0·346
$S = \frac{\Sigma_1}{D_2 (p_1^2 - p_2^2)}$ ..	−0·37 (†)	0·398

† For impure Graphite these values are different.

HETEROCYCLIC COMPOUNDS*

Part II. Synthesis of 4-Quinazolones with Substituents in the 2- and 3-positions

By M. R. Subbaram

(*University of Madras, Madras*-25)

Received January 21, 1954

(Communicated by Dr. K. N. Menon, F.A.SC.)

Methods previously employed for the preparation of 4-quinazolones include, among others, the treatment of N-acylanthranilides to elevated temperatures[1] or treatment of acylanthranils with primary amines.[2] McKee, McKee and Bost[3] employed the action of substituted benzonitriles with acid chlorides to get 2-substituted-4-quinazolones. 2:3-substituted-4-quinazolones were obtained by Grimmel, Guenther and Morgan[4] by a method which allows the preparation of these compounds in one simple operation at moderate temperatures. When primary amines are condensed with N-acetylanthranilic acid in toluene or any other suitable solvent, with the aid of phosphorus trichloride, 4-quinazolones are formed in fairly good yield.

As part of a scheme of study of Heterocyclic Compounds in progress in this laboratory, the synthesis of some 4-quinazolones (see experimental section) was taken up. While this work was nearing completion, Rani, Vig, Gupta and Narang[5] published a paper on similar lines, embodying the synthesis of several 2:3-substituted-4-quinazolones. The 2:3-substituted-4-quinazolones reported in the present work have a methyl group in position 2, and a substituted aryl group in position 3. The N-acetylanthranilic acid required for this work was most satisfactorily obtained by the method of Bogert and Gotthelf.[6]

Experimental

2-Methyl-3-(2'-chloro-4'-nitrophenyl)-4-quinazolone.—In a 500 ml. three-necked flask equipped with stirrer, reflux condenser and dropping funnel, and mounted in an oil-bath, were placed 1·8 g. (0·01 mole) of N-acetylanthranilic acid, 1·7 g. (0·01 mole) of 2-chloro-4-nitroaniline and 75 ml.

* Part I. Menon and Raman, *Proceedings*, 1953, **38A**, 132.

of dry toluene. The mixture was stirred and treated drop by drop with a solution of 0·5 g. (0·0034 mole) of phosphorus trichloride in 5 ml. of toluene over a period of five minutes. The resulting suspension was stirred and refluxed for two hours. After cooling, the contents of the flask were transferred to a round-bottomed flask, treated with 100 ml. of a 10% sodium carbonate solution and steam distilled, to remove toluene. The residue was collected and crystallised from acetone giving 1·7 g. (63% yield) of the quinazolone, m.p. 170–71°. ($C_{15}H_{10}O_3N_3Cl$: Calculated—N, 13·31. Found: 13·35).

2-*Methyl*-3-(2′-*methyl*-5′-*chlorophenyl*)-4-*quinazolone*.—Condensation of 1·8 g. (0·01 mole) of N-acetylanthranilic acid with 1·4 g. (0·01 mole) of 2-methyl-5-chloroaniline gave 2·0 g. of the pure quinazolone (from acetone), m.p. 142–44°. ($C_{16}H_{13}ON_2Cl$: Calculated—N, 9·84. Found: 9·59).

2-*Methyl*-3-(2′:6′-*dimethylphenyl*)-4-*quinazolone*.—N-acetylanthranilic acid (1·8 g., 0·01 mole) and 2:6-dimethyl aniline (1·2 g., 0·01mole) gave 1·8 g. of the pure quinazolone (from acetone), m.p. 130–32° ($C_{17}H_{16}ON_2$: Calculated—N, 10·60. Found: 10·54).

2:6-*Dimethyl*-3-(o-*tolyl*)-4-*quinazolone*.—Molar proportions of N-acetyl-5-methyl anthranilic acid[7] (2·0 g.) and *o*-toluidine (1·0 g.) gave 1·0 g. of the pure quinazolone (from acetone), m.p. 159–61° ($C_{17}H_{16}ON_2$: Calculated—N, 10·60. Found: 10·59).

2:6-*Dimethyl*-3-(o-*anisyl*)-4-*quinazolone*.—Molar proportions of N-acetyl-5-methyl anthranilic acid (2·0 g.) and *o*-anisidine (1·2 g.) gave 1·8 g. of the pure quinazolone (from acetone), m.p. 176–78° (Calculated for $C_{17}H_{16}O_2N_2$: N, 10·00. Found: 10·18).

2:6-*Dimethyl*-3-(o-*phenetyl*)-4-*quinazolone*.—Molar proportions of N-acetyl-5-methyl anthranilic acid (2·0 g.) and *o*-phenetidine (1·3 g.) gave 2·1 g. of the pure quinazolone (from acetone), m.p. 138–40°. ($C_{18}H_{18}ON_2$: Calculated—N, 9·53. Found: 9·53).

I wish to take this opportunity to express my thanks to Dr. K. N. Menon for his interest and guidance during the course of this work.

Summary

The synthesis of 2-methyl-3-aryl-4-quinazolones is reported.

REFERENCES

1. Körner .. *J. Prakt. Chem.*, 1887, **36** (2), 165.
2. Bogert and Chambers .. *J. Amer. Chem. Soc.*, 1905, **27**, 649.
   ——— and May .. *Ibid.*, 1909, **31**, 512.
   Anschütz, Schmidt and Greiffenberg .. *Ber.*, 1902, **35**, 3482.
3. McKee, McKee and Bost .. *J. Amer. Chem. Soc.*, 1947, **69**, 940.
4. Grimmel, Guenther and Morgan .. *Ibid.*, 1946, **68**, 542.
5. Rani, Vig, Gupta and Narang .. *J. Ind. Chem. Soc.*, 1953, **30**, 331.
6. Bogert and Gotthelf .. *J. Amer. Chem. Soc.*, 1900, **22**, 534.
7. Hayashi, Tsuruoka, Morikawa and Namikawa *Bull. Chem. Soc. Japan*, 1936, **11**, 184.

GENERALIZED SINGULAR POINTS WITH APPLICATIONS TO FLOW PROBLEMS*

By B. R. Seth, F.A.Sc.

(Indian Institute of Technology, Kharagpur)

Received November 28, 1953

Summary

Generalized singular points are used to discuss irrotational and viscous flows produced in an infinite liquid by a moving solid. It is found that the irrotational motion of translation is the same as that due to a generalized doublet and that of rotation the same as that due to a " rotation singular point". The corresponding viscous problems are solved by superposing on the irrotational motion a solution due to a concentrated force or a couple.

1. Introduction

Singular points play an important part in all branches of mathematics. They appear as sources, sinks, doublets, rectilinear vortices, electric charges, magnetic particles, electric currents, etc. It is customary to think of them as the limiting cases of spherical or circular elements. It is well known that all potential flow can be produced by a suitable distribution of them. But, excepting for simple boundaries like planes, spheres or circles, this distribution is infinite in number, and, hence for practical applications it is not very suitable. It is not generally appreciated that a generalization of these points as ultimate forms of a family of closed surface bodies can simplify a large number of boundary problems by reducing the infinite number of spherical or circular points to a finite number of generalized singular points. For example, an ellipsoidal source or doublet can play the same part for ellipsoidal boundaries as an ordinary source or doublet does for spherical boundaries. In fact the uniform non-viscous flow due to the motion of an ellipsoid can be produced by an ellipsoidal doublet.

It is proposed to discuss how such generalized singular points may be obtained and used for flow problems. It is found that:—

(i) the irrotational motion of a solid through a non-viscous liquid is the same as that due to a generalized doublet;

* Presented at the Eighth International Congress on Theoretical and Applied Mechanics held in Istanbul, 1952.

(ii) the irrotational motion of rotation is the same as that due to "a rotation singular point";

(iii) the slow viscous motion of the solid can be obtained by superposing on an irrotational motion due to a generalized doublet a solution due to a concentrated force in the direction of motion;

(iv) the slow viscous motion due to rotation of the solid, if stable, can be obtained by superposing on the motion due to "a rotation singular point," the solution due to "a centre of rotation".

The corresponding analogies in electricity and magnetism and heat conduction can be easily written down.

2. IRROTATIONAL FLOW

Let us take a family of closed surfaces given by

$$f(x, y, z, \xi) = 0, \tag{1}$$

and let us assume that the surface of the moving solid A is given by $\xi = \xi_0$. The family given by ξ = a constant, is not necessarily a family of equipotential surfaces. In order that it be so we should have

$$\nabla^2 [F(\xi)] = 0, \tag{2}$$

which gives that[1]

$$\nabla^2 \xi \Big/ \left[\left(\frac{\partial \xi}{\partial X}\right)^2 + \left(\frac{\partial \xi}{\partial y}\right)^2 + \left(\frac{\partial \xi}{\partial z}\right)^2\right]$$

should be a function of ξ only, say $\psi'(\xi)$. When this condition is satisfied the corresponding potential is found to be

$$c \int \exp [-\psi(\xi)]\, d\xi + d \tag{3}$$

c and d being constants.

Let V be the potential at an external point due to the solid A whose mass is M. Then, by Gauss' theorem the normal flux across any surface enclosing S is

$$\iint_S -\frac{\partial V}{\partial n}\, ds = -4\pi M,$$

the element of normal δn being drawn outwards. The limiting form of A when it reduces to a point or a line will be called the generalized source of strength M. Its potential will be taken as V. V satisfies the following conditions:—

(i) $\nabla^2 V = 0$ throughout all space unoccupied by matter;

(ii) the flow across any closed surface containing it is constant;

(iii) Grad. V vanishes at infinity. The generalized source thus satisfies all the requisite conditions.

A doublet in the x-direction is obtained by displacing the source or solid through a small distance in the x-direction. The corresponding potential is $\mu\, \partial V/\partial x$, μ being the strength of the doublet. Again, the composite body whose density at any point Q is the difference of the densities at Q of the given body in two neighbouring positions is equivalent to a boundary layer of density $\rho \cos \theta$ placed on the surface of the solid A, θ being the angle which the normal makes with the x-axis. Thus the doublet can be taken to be equivalent to a boundary layer on the surface of A of surface density $\rho \cos \theta$.

If, instead of giving a translatory displacement, we turn the body round the z-axis through a small angle, we get a " rotation singular point ", whose potential

$$\phi = \mu \left(x \frac{\partial V}{\partial y} - y \frac{\partial V}{\partial x} \right), \tag{4}$$

is the same as that of a boundry layer on the surface of A of surface density $\mu(mx - ly)$, l, m, n being the direction cosines of the normal to the surface S of the body A.

We shall now show how these singular points may be used to discuss the motion due to the translation and rotation of the solid A in an infinite non-viscous liquid.

At first we show that a generalized doublet or boundary layer gives the flow due to the motion of the solid A through an infinite non-viscous liquid.

By Green's theorem, if N, N′ are the normal intensities due to the boundary layer of density $\rho \cos \theta$ at points just inside and just outside the layer, we have

$$N' - N = 4\pi\rho \cos \theta. \tag{5}$$

Now, since the surface S is an equipotential, we can take $N = 0$. Thus we see that the normal component of the potential due to the doublet assumes a value proportional to $\cos \theta$, which is the condition to be satisfied by the potential in the corresponding irrotational motion. The constants can be easily adjusted in terms of the velocity of the solid A.

We have thus shown that the motion of the solid A through an infinite non-viscous liquid can be represented by a generalised doublet, whose potential can be obtained from the static potential due to the solid A.

In the case of a sphere moving through an infinite liquid we have the following results:—

The potential V at any external point is

$$\frac{M}{r}.$$

The potential due to the corresponding doublet is

$$\phi = -\mu \frac{\partial}{\partial x}\left(\frac{1}{r}\right) = \frac{\mu x}{r^3},$$

which is the known result for the potential of liquid flow.

In like manner for a circular cylinder we have

$$V = c - 2M \log r,$$

so that

$$\phi = \frac{\mu x}{r^2},$$

which is again a known result.

Let us take the case of an ellipsoid. The confocal family of ellipsoids is given by

$$\frac{x^2}{a^2+\lambda} + \frac{y^2}{b^2+\lambda} + \frac{z^2}{c^2+\lambda} = 1.$$

The potential due to an ellipsoidal source is[2]

$$V = \int_{\lambda}^{\infty} \left(1 - \frac{x^2}{a^2+u} - \frac{y^2}{b^2+u} - \frac{z^2}{c^2+u}\right) \frac{du}{\Delta}. \tag{6.1}$$

The potential of the ellipsoidal doublet is therefore given by

$$\phi = -\mu \frac{\partial V}{\partial x} = \mu_1 x \alpha, \tag{6.2}$$

μ_1, being a constant, and Δ, α are given by

$$\Delta = [(a^2+u)(b^2+u)(c^2+u)]^{\frac{1}{2}}, \quad \alpha = \int_{\lambda}^{\infty} \frac{du}{(a^2+u)\Delta}, \tag{6.3}$$

which result is again known.

For an elliptic cylinder we have[3]

$$V = -2\pi\rho \frac{ab}{a'+b'}\left(\frac{x^2}{a'} + \frac{y^2}{b'}\right) - 2\pi\rho ab \log(a'+b') + c \qquad (7.1)$$

a', b' being the axes of the confocal ellipse through the attracted point. This value of V gives

$$\phi = \mu \frac{ab}{a'+b'} \frac{x}{a'}, \quad a' = c\cosh\xi, \quad b' = c\sinh\xi,$$

$$x = c\cosh\xi\cos\eta, \quad y = c\sinh\xi\sin\eta. \qquad (7.2)$$

Substituting these values we get the known result

$$\phi = \mu_1 \exp(-\xi)\cos\eta.$$

For the elliptic source V is of the form[4]

$$V = -\tfrac{1}{2}\pi\rho ab\,(e^{-2\xi}\cos 2\eta + 2\xi). \qquad (7.3)$$

For the motion of rotation, we easily get the following known results for the value of ϕ given in (4) :—

(i) for a sphere or a circular cylinder $\phi = 0$;

(ii) for an ellipsoid* $\phi = \mu_1(\beta - \alpha)\,xy$,

(iii) for an elliptic cylinder $\phi = \mu_1 e^{-2\xi}\sin 2\eta$. (8)

Thus we see that the irrotational motion of an infinite liquid due to the translation or rotation of the solid A can be easily deduced from the static potential of the body at any external point, by using the idea of generalised singular points.

For any internal point V satisfies Poisson's equation

$$\nabla^2 V = -4\pi\rho \text{ or } -2\pi\rho \qquad (9)$$

according as it is a three-dimensional or two-dimensional problem. ρ is assumed to be a constant, and hence V does not satisfy Laplace's equation. But its first partial derivatives with respect to x, y, z satisfy it. The potential for the transational and rotational flows of the liquid contained in the surface S of the body A remain of the form

$$\mu \frac{\partial V}{\partial x} \text{ and } \mu\left(x\frac{\partial V}{\partial y} - y\frac{\partial V}{\partial x}\right). \qquad (10)$$

* β is obtained from α in (6.3) by interchanging a and b.

The following results now follow immediately:—

(1) for the motion of translation along the x-axis of any solid $\phi = -Ux$

(2) for the rotation of sphere or circular cylinder $\phi = 0$;

(3) for rotation of an ellipsoid, we have to use $V = D - Ax^2 - By^2 - Cz^2$, D, A, B, C being constants. This gives

$$\phi = \mu_1 xy$$

(4) for an elliptic cylinder

$$V = D - 2\pi\rho \frac{ab}{a+b}\left(\frac{x^2}{a} + \frac{y^2}{b}\right), \quad \phi = \mu_1 xy.$$

Thus liquid motion contained in a closed surface given by (1) can be deduced from the static potential at any point inside the body A.

3. Viscous Flow

For the slow motion of a solid through a viscous liquid we have to consider generalised singular points of various types. In the first type we determine the displacements produced in an infinite elastic solid wherein a concentrated force X_0 acts at the origin in the direction of the X-axis. In this case we know that the displacements components can be put in the form[5]

$$u = \frac{\partial \phi}{\partial x} + \frac{\partial H}{\partial y} - \frac{\partial G}{\partial z}, \text{ etc.} \tag{11.1}$$

and the body force X, Y, Z in the form

$$X = \frac{\partial \Phi}{\partial x} + \frac{\partial N}{\partial y} - \frac{\partial M}{\partial z}, \text{ etc.} \tag{11.2}$$

where

$$(\lambda + 2\mu)\nabla^2\phi + \rho\Phi = 0, \ \mu\nabla^2 F + \rho L = 0, \ \mu\nabla^2 G + \rho M = 0,$$
$$\mu\nabla^2 H + \rho N = 0. \tag{12}$$

The Laplace's equation in orthogonal curvilinear co-ordinates ξ, η, ξ is

$$\frac{\partial}{\partial \xi}\left(\frac{h_1}{h_2 h_3}\frac{\partial V}{\partial \xi}\right) + \text{two similar terms} = 0,$$

where

$$\frac{1}{h_1^2} = \left(\frac{\partial x}{\partial \xi}\right)^2 + \left(\frac{\partial \gamma}{\partial \xi}\right)^2 + \left(\frac{\partial z}{\partial \xi}\right)^2, \text{ etc.} \tag{13}$$

Let the surface of the moving solid A be given by the equipotential $\xi = \xi_0$. There is a solution of (13) which is a function of ξ only. Let it be

denoted by $\psi(\xi)$. It should be such, that its flux across any equi-potential surface is equal to 4π in three dimensions and 2π in two dimensions.

Putting

$$\rho \int\int\int X'\, dx'dy'dz' = X_0,$$

we get[5]

$$\Phi = -\frac{1}{4\pi\rho} X_0 \frac{\partial\psi}{\partial x},\ L=0,\ M=\frac{1}{4\pi\rho} X_0 \frac{\partial\psi}{\partial z},\ N=-\frac{1}{4\pi\rho} X_0 \frac{\partial\psi}{\partial y}. \tag{14}$$

Since

$$\nabla^2(x\psi) = 2\frac{\partial\psi}{\partial x},$$

we can put

$$\phi = \frac{X_0}{8\pi(\lambda+2\mu)} x\psi,\ F=0,\ G=-\frac{X_0}{8\pi\mu} z\psi,$$

$$H=\frac{X_0}{8\pi\mu} y\psi. \tag{15}$$

u, v, w now take the form

$$u = -\frac{(\lambda+\mu)X_0}{8\pi\mu(\lambda+2\mu)} \frac{\partial}{\partial x}(x\psi) + \frac{X_0}{4\pi\mu}\psi,$$

$$v, w = -\frac{(\lambda+\mu)X_0}{8\pi\mu(\lambda+2\mu)} \left(\frac{\partial}{\partial y}, \frac{\partial}{\partial z}\right)(x\psi). \tag{16}$$

These give

$$\Delta = \frac{\partial u}{\partial x} + \frac{\partial v}{\partial y} + \frac{\partial w}{\partial z} = \frac{X_0}{4\pi(\lambda+2\mu)} \frac{\partial\psi}{\partial x}, \tag{17.1}$$

$$\tau_{xx} = \frac{(3\lambda+4\mu)X_0}{4\pi(\lambda+2\mu)} \frac{\partial\psi}{\partial x} - \frac{(\lambda+\mu)X_0}{4\pi(\lambda+2\mu)} \frac{\partial^2}{\partial x^2}(x\psi)$$

$$\tau_{yz} = -\frac{(\lambda+\mu)X_0}{4\pi(\lambda+2\mu)} \frac{\partial^2}{\partial y\partial z}(x\psi),\ \text{etc.} \tag{17.2}$$

The equations of equilibrium are satisfied with these values of τ_{xx}, τ_{yz}, etc. They have to satisfy the condition that across any surface $\xi = \text{constant}$, they give a force X_0 in the x direction, independent of ξ.

X_γ, the traction component along the x-axis is

$$X_\gamma = l\tau_{xx} + m\tau_{xy} + n\tau_{xz}$$

$$= -\frac{(\lambda+\mu)X_0}{4\pi(\lambda+2\mu)} \left[l\frac{\partial^2}{\partial x^2} + m\frac{\partial^2}{\partial x\partial y} + n\frac{\partial^2}{\partial x\partial z}\right](x\psi)$$

$$+ \frac{X_0}{4\pi}\left(l\frac{\partial}{\partial x} + m\frac{\partial}{\partial y} + n\frac{\partial}{\partial z}\right)\psi + \frac{\lambda+\mu}{2\pi(\lambda+2\mu)} X_0 \frac{\partial\psi}{\partial x}, \tag{18.1}$$

l, m, n being the direction cosines of the normal drawn to $\xi = \text{constant}$. If $\delta\gamma$ is an element of this normal we can write (18.1) as

$$X_\gamma = -\frac{(\lambda+\mu)\,X_0}{4\pi(\lambda+2\mu)}\,x\,\frac{\partial}{\partial\gamma}\left(\frac{\partial\psi}{\partial x}\right) + \frac{\mu X_0}{4\pi(\lambda+2\mu)}\,\frac{\partial\psi}{\partial\gamma} + \frac{(\lambda+\mu)\,X_0}{4\pi(\lambda+2\mu)}\,l\,\frac{\partial\psi}{\partial x}. \tag{18.2}$$

We shall now show that

$$\iint X_\gamma ds = X_0,$$

the integration being taken over any closed surface $\xi = \text{constant}$.

We shall assume that the liquid is bounded by the surface $S\,(\xi = \xi_0)$ and an equipotential surface at infinity given by $\xi = \infty$. In the usual notation

$$\iint_s X_\gamma ds = \iint X_\gamma ds - \iint_\infty X_\gamma ds. \tag{19.1}$$

But X_γ is given by (18.2). Also

$$\begin{aligned}\iint_s x\,\frac{\partial}{\partial\gamma}\left(\frac{\partial\psi}{\partial x}\right)ds - \iint_\infty x\,\frac{\partial}{\partial\gamma}\left(\frac{\partial\psi}{\partial x}\right)ds &= \iint_s \frac{\partial\psi}{\partial x}\,\frac{\partial x}{\partial\gamma}\,ds - \iint \frac{\partial\psi}{\partial x}\,\frac{\partial x}{\partial\gamma}\,ds \\ &= \iint_s l\,\frac{\partial\psi}{\partial x}\,ds - \iint_\infty l\,\frac{\partial\psi}{\partial x}\,ds \end{aligned} \tag{19.2}$$

But, since $\psi \to 1/r$, at infinity, we have

$$\iint_\infty x\,\frac{\partial}{\partial\gamma}\left(\frac{\partial\psi}{\partial x}\right)ds = \frac{8}{3}\pi, \quad \iint_\infty l\,\frac{\partial\psi}{\partial x}\,ds = -\frac{4}{3}\pi.$$

Hence

$$\iint_s x\,\frac{\partial}{\partial\gamma}\left(\frac{\partial\psi}{\partial x}\right)ds = \iint_s l\,\frac{\partial\psi}{\partial x}\,ds + 4\pi. \tag{19.3}$$

Similarly

$$\iint_s \frac{\partial\psi}{\partial\gamma}\,ds - \iint_\infty \frac{\partial\psi}{\partial\gamma}\,ds = 0,$$

so that

$$\iint_s \frac{\partial\psi}{\partial\gamma}\,ds = -4\pi. \tag{19.4}$$

Thus

$$\iint_s X_\gamma \, ds = -\frac{X_0 \mu}{\lambda + 2\mu} - \frac{X_0 (\lambda + \mu)}{\lambda + 2\mu} = -X_0, \tag{19.5}$$

which shows that a force X_0 should be applied in the x-direction. Similarly

$$\begin{aligned} Y_\gamma &= -\frac{(\lambda+\mu) X_0}{4\pi(\lambda+2\mu)} \, x \, \frac{\partial}{\partial \gamma}\left(\frac{\partial \psi}{\partial y}\right) + \frac{(\lambda+\mu) X_0}{4\pi(\lambda+2\mu)} \, m \, \frac{\partial \psi}{\partial x}, \\ Z_\gamma &= -\frac{(\lambda+\mu) X_0}{4\pi(\lambda+2\mu)} \, x \, \frac{\partial}{\partial \gamma}\left(\frac{\partial \psi}{\partial z}\right) + \frac{(\lambda+\mu) X_0}{4\pi(\lambda+2\mu)} \, n \, \frac{\partial \psi}{\partial x} \end{aligned} \tag{19.6}$$

from which we easily see that

$$\iint_s Y_\gamma \, ds = 0, \quad \iint_s Z_\gamma \, ds = 0.$$

For the vanishing of the couple we should have

$$\iint_s (z Y_\gamma - y z_\gamma) \, ds = 0, \tag{20}$$

or

$$\iint_s \left[\frac{\partial \psi}{\partial y}(lz + nx) - \frac{\partial \psi}{\partial z}(ly + mx) - ny \frac{\partial \psi}{\partial y} - mz \frac{\partial \psi}{\partial x}\right] ds = 0.$$

Transforming into volume integrals, we see that this condition is also satisfied.

For a liquid $\triangle \to 0$, $\lambda \to \infty$, such that $\lambda \triangle \to -p$. Thus we get from (16)

$$\tau_{xx} = -p + 2\mu B \left[\frac{\partial^2}{\partial x^2}(x\psi) - 2\frac{\partial \psi}{\partial x}\right],$$

$$\tau_{yy} = -p + 2\mu B \frac{\partial^2}{\partial y^2}(x\psi),$$

$$\tau_{zz} = -p + 2\mu B \frac{\partial^2}{\partial z^2}(x\psi),$$

$$\tau_{yz} = 2\mu B \frac{\partial^2}{\partial y \partial z}(x\psi), \quad \tau_{zx} = 2\mu B \frac{\partial^2}{\partial x \partial z}(x\psi) - 2\mu B \frac{\partial \psi}{\partial z} \tag{21.1}$$

$$\tau_{xy} = 2\mu B \frac{\partial^2}{\partial x \partial y}(x\psi) - 2\mu B \frac{\partial \psi}{\partial y}, \tag{21.2}$$

where $\nabla^2 \psi = 0$ and $B = -X_0/8\pi\mu$.

The tractions become

$$X_\gamma = 2\mu B\left[l\frac{\partial^2}{\partial x^2} + m\frac{\partial^2}{\partial x\partial y} + n\frac{\partial^2}{\partial x\partial z}\right](x\psi)$$

$$- 2\mu B\left(l\frac{\partial}{\partial x} + m\frac{\partial}{\partial y} + n\frac{\partial}{\partial z}\right)\psi - lp \qquad (21.3)$$

$$= 2\mu Bx\frac{\partial}{\partial\gamma}\left(\frac{\partial\psi}{\partial x}\right) - lp,$$

$$Y_\gamma,\ Z_\gamma = 2\mu Bx\frac{\partial}{\partial\gamma}\left(\frac{\partial\psi}{\partial y}, \frac{\partial\psi}{\partial z}\right).$$

The displacement u, v, w take the form

$$u = B\left[\frac{\partial}{\partial x}(x\psi) - 2\psi\right],$$

$$v, w = B\left(\frac{\partial}{\partial y}, \frac{\partial}{\partial z}\right)(x\psi). \qquad (21.4)$$

Let V be the potential of the corresponding irrotational flow. On the boundary of the moving solid ($\xi =$ constant) we have

$$-h_1\frac{\partial V}{\partial\xi} = h_1 U\frac{\partial x}{\partial\xi}, \text{ or } \frac{\partial V}{\partial\xi} = -U\frac{\partial x}{\partial\xi}. \qquad (22)$$

If V is of the form $x\alpha(\xi)$, the velocities for the slow viscous motion can be at once obtained by superposing on the generalized doublet of the corresponding irrotational motion a generalized singular point of the first type. Thus we get

$$u = A\frac{\partial V}{\partial x} - \frac{X_0}{8\pi\mu}\left[\frac{\partial}{\partial x}(\partial\psi) - 2\psi\right],$$

$$v = A\frac{\partial V}{\partial y} - \frac{X_0}{8\pi\mu}\frac{\partial}{\partial y}(\psi), \qquad (23)$$

$$w = A\frac{\partial V}{\partial z} - \frac{X_0}{8\pi\mu}\frac{\partial}{\partial z}(x\psi),$$

where the constant A can be determined from the boundary conditions.

If the irrotational motion is represented by harmonics of the type V_n, V in (23) will have V_n and all harmonies of an order less than V_n.

When $V = x\alpha(\xi)$ we get from (22)

$$A\left[\alpha_0 + x\alpha_0'\frac{\partial\xi}{\partial x}\right] - \frac{X_0}{8\pi\mu}\left[x\psi_0'\frac{\partial\xi}{\partial x} - \psi_0\right] = U \qquad (24)$$

where a_0, ψ_0 are the values of a, ψ on the surface of the solid, dashes denote differentiation with respect to ξ, and U is the uniform velocity of the solid A. Thus

$$A\,a_0 + \frac{X_0\psi_0}{8\pi\mu} = U,\ A\,a_0' = \frac{X_0\psi_0'}{8\pi\mu}\cdot \tag{25.1}$$

These values of X_0 and A also ensure that $v=0$, $w=0$ on the boundary. The drag suffered by the solid and the constant A are given by

$$X_0 = \frac{8\pi\mu\, a_0' U}{\psi_0 a_0' + \psi_0' a_0},\ A = \frac{\psi_0'}{\psi_0 a_0' + \psi_0' a_0}\cdot \tag{25.2}$$

The second case when V is to be represented by a series of harmonics can be similarly treated.

In the particular case of the sphere we get

$$V = xa = \frac{2}{3}\frac{x}{r^3},\ \psi = \frac{1}{r},\ A = \frac{3}{8}a^3,\ X_0 = 6\pi a\mu U. \tag{26}$$

These give the known values of u, v, w

For a circular cylinder we get[6]

$$V = x\,a = \frac{x}{r^2},\ \psi = -\log r,$$

$$X_0 = \frac{4\pi\mu\, a_0' U}{\psi_0 a_0' + \psi_0' a_0} = \frac{8\pi\mu\, U}{1 - 2\log a}\cdot \tag{27}$$

An infinite constant is neglected in the value of ψ, which is a well-known drawback.

For an elliptic cylinder we have

$$a = e^{-\xi}\ \text{sech}\ \xi,\ \psi = -\xi \tag{7}$$

$$X_0 = \frac{4\pi\mu\, U\,(a+b)}{a - \xi_0(a+b)},$$

$$a = c\cosh\xi_0,\ b = c\sinh\xi_0,\ c^2 = a^2 - b^2. \tag{28}$$

For an ellipsoid we have the following results:—

$$\psi_0' = -\frac{1}{2abc},\ a_0' = -\frac{1}{a^3bc},\ A = \frac{Ua^2}{2\psi_0 + a^2 a_0}, \tag{29.1}$$

$$X_0 = \frac{16\pi\mu U}{2\psi_0 + a^2 a_0}, \tag{29.2}$$

and the values for u, v, w which are known.[7]

For the slow rotatory motion of a sphere or a cylinder in a viscous liquid we have to use the generalised singular point, called " the centre of rotation". In both cases there is no irrotational motion, and hence we can take $V=0$. For a sphere, if G is the couple of rotation, the corresponding displacements in an incompressible infinite solid are

$$u,\ v=\frac{G}{8\pi\mu}\left(\frac{\partial}{\partial y},\ -\ \frac{\partial}{\partial x}\right)\frac{1}{r},\ w=0 \tag{30.1}$$

If ω_0 is the angular velocity and a the radius of the sphere

$$G=8\pi\mu\, a^3\,\omega_0 \tag{30.2}$$

For a circular cylinder of radius a we get the following results:—

$$u,\ v=\frac{G}{4\pi\mu}\left(-\frac{\partial}{\partial y},\ \frac{\partial}{\partial x}\right)\log r,\ w=0 \tag{31.1}$$

$$G=4\pi\mu a^2\,\omega_0 \tag{31.2}$$

REFERENCES

1. Goursat, E. .. *Mathematical Analysis*, **2**, Part 1, 55.
2. Routh, E. J. .. *Statics*, **2**, 114.
3. ———— .. *Ibid.*, 118.
4. Sharma, P. N. .. *Proc. Benaras Math. Soc.*, 1942, **4**, 32–38.
5. Love, A. E. H. .. *Math. Theory of Elasticity*, Fourth ed. 1927, pp. 183-84.
6. Seth, B. R. .. *Proc. Ind. Acad. Sci.*, 1942, **16A**, 193-95.
7. Lamb, H. .. *Hydrodynamics*, Fifth ed., 1930, p. 572.

ON THE SEMI-EMPIRICAL MASS-FORMULA AND ALPHA-DISINTEGRATION ENERGY IN THE REGION OF HEAVY AND MEDIUM HEAVY NUCLIDES

By G. P. Dube, F.A.Sc. and Lal Saheb Singh

(*Department of Physics, Patna University, Patna*)

Abstract

In the present paper it has been shown that Fermi's semi-empirical atomic mass-formula is inadequate for the estimation of alpha-disintegration energy in the medium heavy and heavy nuclide-regions. A suitable correction-term has been added to the mass-formula based on Duckworth's new atomic masses and similar to the one proposed by Stern for heavy elements ($A \geqslant 208$). It is seen that the calculated alpha-decay energies are in numerical agreement with the observed data except for the magic number nuclei which can be satisfactorily explained on the nuclear shell-structure. But even in the latter case the agreement with the experimental results is better when the correction-term is used.

Introduction

The determination of atomic masses to a high degree of precision is of great importance because of its many significant applications in Nuclear Physics. The binding energy of the nuclei, conditions of nuclear stability, radioactive properties of isotopes, excited states of parent and daughter-nuclei, their inner structural informations, the nature of nuclear forces—all these need directly or indirectly for their estimation sufficiently accurate atomic masses. The discrepancy discovered in any one of them requires significant interpretations. The accuracy obtainable in the most refined mass spectrographic measurements is limited to about 1 part in 10^5, and thus is an error of about 0·01 mass units (M.U.) or 10 Mev. in the region of heavy and medium-heavy nuclides. Since the radioactive decay energies are limited to a few Mev. only, the mass spectrographic data are not of much help in the understanding of the radioactive decay of medium heavy and heavy nuclides. In recent years Duckworth *et al.* (1951) has reported some new atomic mass measurements in which the accuracy in the region of mass numbers 120 to 200 is claimed to be of the order of 0·001 M.U. or about 1 Mev.

Several attempts have been made since 1935 to set up a suitable semi-empirical mass-formula for the estimation of atomic masses when

experimental data are lacking and they have proved of immense help in the understanding of many nuclear properties.

In the last few years more than 100 alpha-emitters have been discovered in the region extending from bismuth ($Z = 83$) to transuranium elements upto $Z = 98$ and in the rare-earth region ($Z = 59$ to $Z = 72$). The systematics of alpha decay properties have been well defined in a paper by I. Perlman, A. Ghiorso and G. T. Seaborg (1950) and the properties of possible alpha-emitters have been predicted.

A number of short-lived alpha-emitters have been observed in the isotopes of gold ($Z = 79$) and mercury ($Z = 80$) (Thompson *et al.*, 1949). Of great interest is the discovery of a number of alpha-emitters in the rare-earth region with half-lives ranging from a few minutes to a few days and alpha-particle energies in the range 4·2 to 2·0 Mev. (Thompson *et al.*, 1949), Weaver (1950), Rasmussen *et al.* (1950 & 1953).

A good test of the reliability of the semi-empirical mass-formula is to calculate the alpha-disintegration energies of a number of nuclides and compare them with the experimentally observed data. Several attempts have been made in this direction and the inadequacies of some of the semi-empirical formulæ in the investigation of the radioactive decay energies have been well established but the position with regard to the correction-term to be added to the semi-empirical formula so as to give better fit with experimental results in the regions of medium-heavy and heavy nuclei has not been clarified.

In what follows, it has been shown that Fermi's semi-empirical formula, with a suitable correction-term which depends on both A and Z, gives reliable estimates of alpha-disintegration energy in the medium-heavy and heavy-nuclide regions except for the magic number nuclei containing 126 neutrons but even in this case the agreement is better. The correction-term has been guessed with the help of Duckworth's new atomic mass-values.

Calculation of alpha-disintegration energy (E_α)

Let us consider an alpha-emitter of atomic mass M (Z, A) and the daughter atom of mass M (Z − 2, A − 4). The alpha-disintegration energy E_α is given by

$$E_\alpha = M(Z, A) - M(Z - 2, A - 4) - M(2, 4) \ldots . \text{M.U.} \quad (1)$$

According to Fermi's semi-empirical mass formula (*Nuclear Physics*, 1951)

$$M(Z, A) = 0{\cdot}99391\, A - 0{\cdot}00085\, Z + 0{\cdot}014\, A^{2/3} + 0{\cdot}083 \times \frac{(A/2 - Z)^2}{A} + 0{\cdot}000627\, Z^2/A^{1/3} + \delta(A, Z)$$

where

$$\delta(A, Z) = 0 \text{ for A odd, Z anything}$$
$$= \mp\, 0{\cdot}036\, A^{-3/4} \text{ for A even, Z } \begin{cases}\text{even}\\ \text{odd}\end{cases} \qquad (2)$$

substituting (2) in (1) E_α in Mev. is given by

$$E_\alpha = -27{\cdot}90728 + 13{\cdot}03610\,\{A^{2/3} - (A-4)^{2/3}\} - 77{\cdot}28545 \times \frac{(A-2Z)^2}{A(A-4)} + 0{\cdot}58383\left\{\frac{Z^2}{A^{1/3}} + \frac{(Z-2)^2}{(A-4)^{1/3}}\right\} + 931{\cdot}15 \times \times \{\delta(A, Z) - \delta(A-4, Z-2)\} \qquad (3)$$

The last term in (3) is zero for A odd, Z anything and $= \pm\, 33{\cdot}52140$

$$\times \{(A-4)^{-3/4} - A^{-3/4}\} \text{ for A even, Z } \begin{cases}\text{even}\\ \text{odd}\end{cases}$$

(1) *Heavy nuclides.*—The formula has been used for the calculation of E_α in the isotopes of the heavy elements for Z = 96 to Z = 83 and the results are given in the Table I.

It is seen that in every case the calculated E_α comes lower than the observed one. For isotopes of a given element, E_α is found to increase linearly with the decrease in the mass number A, the rate of increase being nearly the same for isotopes of different elements, *i.e.*, it is independent of Z.

For a given A, the calculated E_α is found to increase with the increase of Z and the rate of increase is nearly the same for all values of A ranging from 197 to 246.

The observed E_α shows a general trend of increasing with decrease of A (except in the neighbourhood of completed neutron and proton sub-shells where there is a sudden drop in E_α on the lower side of A containing less than 126 neutrons [Perlman *et al.* (1950)]). The rate of increase depends on A and gradually decreases for higher values of A and Z.

The difference $E_{\alpha obs.} - E_{\alpha cal.}$ has been plotted against A. It is clear from the graph that this difference at first decreases slowly with increasing A but for A $\geq$ 209 it shoots up abruptly—a maximum occurring for A = 211, 212 and 213 for Bi, Po and At respectively (region for N = 126 —completed neutron-subshell). Then it decreases rapidly as A increases. In the transuranium elements, the difference is of the order of 1 Mev. or even less.

(2) *Medium-heavy nuclides.*—There have been observed a number of short-lived alpha-emitters in highly neutron deficient isotopes produced on

TABLE I

Nuclides	Half-lives	Observed $E_\alpha \times \frac{A}{A-4}$ in Mev.	Estimated E_α in Mev.	Difference	Estimated E_α with the correction-term in Mev.
$_{96}Cm^{246}$	..	..	4·762	..	5·894
Cm^{244}	..	6·00	5·062	·938	6·196
Cm^{243}	..	..	5·200	..	6·336
Cm^{242}	150*d*	6·28	5·328	·952	6·465
Cm^{241}	55*d*	..	5·480	..	6·619
Cm^{240}	26·8*d*	6·48	5·590	·890	6·990
Cm^{238}	2·5*h*	6·61	5·850	·760	6·998
$_{95}Am^{242}$	400*y*	5·49	4·763	·727	5·880
Am^{241}	590*y*	5·68	4·911	·769	6·030
Am^{240}	50*h*; 53*h*	..	5·051	..	6·173
Am^{239}	12*h*	5·97	5·188	·782	6·312
Am^{238}	1·5*h*	..	5·333	..	6·460
$_{94}Pu^{241}$	~10*y*	5·19	4·352	·838	5·372
Pu^{240}	~6000*y*	5·29	4·494	·796	5·534
Pu^{239}	24000*y*	5·33	4·636	·694	5·699
Pu^{238}	92*y*	5·70	4·785	·915	5·875
Pu^{236}	2·7*y*	5·96	4·953	1·007	6·062
Pu^{234}	8·5*h*	6·37	5·232	1·138	6·346
Pu^{232}	22*m*	6·71	5·513	1·197	6·633
$_{93}Np^{237}$	$2·2\times10^6$*y*	4·93	4·357	·573	5·449
Np^{235}	435*d*	5·24	4·643	·597	5·738
Np^{233}	35*m*	5·63	4·924	·706	6·118
Np^{231}	53*m*	6·39	5·206	1·186	6·307
$_{92}U^{238}$	$4·51\times10^9$*y*	4·32	3·646	·674	4·729
U^{236}	$2·46\times10^7$*y*	4·58	3·935	·645	5·020
U^{235}	$8·91\times10^8$*y*	4·72	4·077	·643	5·163
U^{234}	$2·35\times10^5$*y*	4·92	4·231	·689	5·319
U^{233}	$1·6\times10^5$*y*	4·99	4·372	·618	5·461
U^{232}	70*y*	5·49	4·512	·978	5·606
U^{231}	4·2*d*	5·70	4·654	1·046	5·750
U^{230}	20·8*d*	6·07	4·828	1·242	5·927
U^{229}	58*m*	6·65	4·940	1·710	6·044
U^{228}	9·3*m*	6·95	5·084	1·866	6·193
$_{91}Pa^{231}$	$3·43\times10^4$*y*	5·19	4·072	1·118	5·130
Pa^{230}	17·7*d*	5·60	4·225	1·375	5·285
Pa^{229}	1·5*d*	5·89	4·377	1·513	5·440
Pa^{228}	22*h*	6·31	4·520	1·790	6·648
$_{91}Pa^{227}$	38*m*	6·69	4·666	2·024	6·798
Pa^{226}	1·7*m*	7·05	4·811	2·249	6·961

TABLE I (*Continued*)

Nuclides	Half-lives	Observed $E_\alpha \times \frac{A}{A-4}$ in Mev.	Estimated E_α in Mev.	Difference	Estimated E_α with the correction-term in Mev.
$_{90}Th^{232}$	$1{\cdot}39\times10^{10}y$	4·12	3·386	·734	4·427
Th^{230}	$8{\cdot}0\times10^{4}y$	4·84	3·676	1·164	4·720
Th^{229}	$7000y$	5·23	3·807	1·423	4·853
Th^{228}	$1{\cdot}90y$	5·62	3·954	1·666	6·048
Th^{227}	$18{\cdot}6d$	6·27	4·101	2·169	6·203
Th^{226}	$30{\cdot}9m$	6·53	4·247	2·283	6·355
Th^{225}	$7{\cdot}8m$	6·70	4·394	2·306	6·506
Th^{224}	Very short	7·33	4·540	2·770	6·658
$_{89}Ac^{228}$	$6{\cdot}13y$	4·62	3·375	1·245	5·425
Ac^{227}	$21{\cdot}7y$	5·13	3·525	1·605	5·579
Ac^{225}	$10{\cdot}0d$	6·01	3·827	2·184	5·889
Ac^{224}	$2{\cdot}9h$	6·39	3·973	2·417	6·043
Ac^{223}	$2{\cdot}2m$	6·82	4·118	2·702	6·192
Ac^{222}	Short	7·09	4·263	2·827	6·343
$_{88}Ra^{226}$	$1622y$	4·97	3·091	1·879	5·128
Ra^{224}	$3{\cdot}64d$	5·89	3·392	2·498	5·430
Ra^{223}	$11{\cdot}2d$	5·93	3·536	2·394	5·576
Ra^{222}	$38s$	6·74	3·685	3·055	5·727
Ra^{221}	$31s$	6·96	3·836	3·124	5·878
Ra^{220}	Short	7·63	3·986	3·644	6·030
$_{87}Fr^{221}$	$4{\cdot}8m$	6·57	3·258	3·312	5·254
Fr^{220}	$27{\cdot}5s$	6·94	3·410	3·530	5·410
Fr^{219}	$\cdot02s$	7·59	3·560	4·030	5·562
Fr^{218}	very short	8·00	3·712	4·288	5·720
Fr^{212}	$19m$	6·49	4·618	1·872	6·650
$_{86}Em^{222}$	$3{\cdot}83d$	5·69	2·521	3·169	4·401
Em^{220}	$54{\cdot}5s$	6·51	2·822	3·688	4·792
Em^{219}	$3{\cdot}92s$	7·07	2·972	4·098	4·992
Em^{218}	$\cdot019s$	7·38	3·124	4·256	5·198
Em^{217}	$10^{-3}s$	8·03	3·276	4·754	5·394
Em^{216}	Very short	8·22	3·427	4·793	5·599
Em^{212}	$23m$	6·42	4·025	2·395	6·395
$_{85}At^{218}$	Several secs.	6·84	2·57	4·270	4·530
At^{217}	$\cdot021s$	7·30	2·72	4·580	4·684
At^{216}	$10^{-3}s$	8·09	2·85	5·240	4·816
At^{215}	$10^{-4}s$	8·31	3·00	5·310	4·968
At^{214}	Very short	8·94	3·150	5·790	5·120
At^{213}	..	9·38	3·300	6·080	5·272

TABLE I (*Continued*)

Nuclides	Half-lives	Observed $E_\alpha \times \frac{A}{A-4}$ in Mev.	Estimated E_α in Mev.	Difference	Estimated E_α with the correction-term in Mev.
At^{212}	$\cdot 25s$	7·52	3·450	4·070	5·424
At^{211}	$7 \cdot 5h$	6·12	3·592	2·528	5·568
$_{85}At^{210}$	..	unobserved	3·743	..	5·719
At^{209}	..	5·76	3·901	1·859	5·879
At^{208}	$4 \cdot 5h$	5·77	4·040	1·730	6·022
At^{207}	$1 \cdot 7h$	5·85	4·192	1·658	6·176
At^{206}	..	unobserved	4·366	..	6·322
At^{205}	..	6·02	4·485	1·535	6·477
At^{204}	..	6·32	4·650	1·670	6·648
At^{203}	..	6·13	4·770	1·360	6·774
At^{202}	..	6·48	4·950	1·530	6·960
At^{201}	..	6·68	5·143	1·537	7·169
$_{84}Po^{218}$	$3 \cdot 05m$	6·23	1·918	4·312	3·798
Po^{216}	$\cdot 158s$	7·02	2·239	4·781	4·131
Po^{215}	$1 \cdot 83 \times 10^{-3}s$	7·64	2·401	5·239	4·299
Po^{214}	$1 \cdot 5 \times 10^{-4}s$	7·97	2·557	5·413	4·461
Po^{213}	$4 \times 10^{-6}s$	8·64	2·681	5·959	4·589
Po^{212}	$3 \cdot 0 \times 10^{-7}s$	9·12	2·868	6·252	4·778
Po^{211}	$5 \times 10^{-3}s$	7·57	3·008	4·562	4·922
Po^{210}	$138d$	5·51	3·181	1·329	5·099
Po^{209}	$200y$	5·12	3·323	1·797	5·243
Po^{208}	$3y$	5·34	3·418	1·922	5·346
Po^{207}	$5 \cdot 7y$	5·30	3·557	1·743	5·495
Po^{206}	$9d$	5·40	3·788	1·612	5·732
Po^{205}	..	5·32	3·932	1·388	5·882
Po^{204}	$4h$	5·56	4·081	1·479	6·041
Po^{203}	$40m$	5·67	4·250	1·420	6·218
Po^{202}	..	6·00	4·366	1·634	6·341
Po^{201}	..	5·82	4·501	1·319	6·483
Po^{200}	..	5·96	4·658	1·302	6·648
$_{83}Bi^{214}$	$19 \cdot 7m$	5·72	1·940	3·780	3·802
Bi^{213}	$47m$	6·09	2·098	3·992	3·964
Bi^{212}	$60 \cdot 5m$	6·32	2·257	4·063	4·127
Bi^{211}	$2 \cdot 16m$	6·87	2·417	4·453	4·293
Bi^{210}	$5 \cdot 0d$	4·95	2·574	2·376	4·456
Bi^{209}	Very short	3·21	2·731	0·479	4·647
Bi^{200}	$62m$	5·61	4·098	1·512	6·028
Bi^{199}	$25m$	5·69	4·242	1·448	6·178
Bi^{198}	$9m$	5·95	4·386	1·564	6·328
Bi^{197}	$2m$	6·43	4·529	1·901	6·479

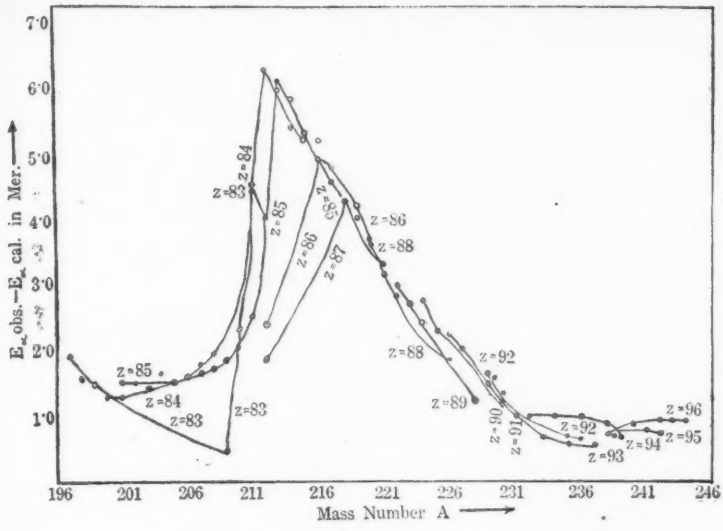

GRAPH

irradiation of gold with high energy deuterons and these have been tentatively assigned to be isotopes of gold and mercury having mass numbers between 185 and 188 (Thompson and Ghiorso, 1949); Rasmussen, 1950; Rasmussen, Thompson and Ghiorso, 1953). The observed alpha-energy in case of gold is 2·20 Mev. and 5·7 Mev. for mercury. These values have slightly been revised but the masses of alpha-emitters have not been deter-

TABLE II

Nuclides	Half-life	Observed $E_\alpha \times \frac{A}{A-4}$ in Mev.	Estimated E_α in Mev.	Difference	Estimated E_α with the correction-term in Mev.
$_{79}Au^{185}$	..	..	4·058	1·122	5·888
Au^{186}	4·3*m*	5·18*	3·960	1·230	5·795
Au^{187}	..	..	3·868	1·312	5·708
Au^{188}	..	..	3·776	1·404	5·621
$_{80}Hg^{185}$	..	..	4·592	1·118	6·476
Hg^{186}	0·7*m*	5·71*	4·453	1·257	6·333
Hg^{187}	..	..	4·308	1·402	6·182
Hg^{188}	..	..	4·150	1·560	6·020

* Masses have been tentatively assigned.

mined conclusively (Rasmussen, Thompson and Ghiorso, 1953). Table II given above shows the observed and calculated E_α and their difference.

The calculated E_α is in every case lower than the observed one and the difference ranges from 1·2 to 1·7 Mev. which is nearly one-third of the calculated values.

Inadequacy.—The general conclusion is that Fermi's formula, though giving reliable estimates in the transuranium elements, is inadequate in other regions. The inadequacy of Bohr-Wheeler (1939) formula and of Bethe-Weizsäcker (1936) has already been established by other workers (Saha and Saha, 1946; Das, 1950; Pryce, 1950). The empirical correction-term due to Stern (1949) which is applicable to $A \geqslant 208$, brings about better numerical agreement for heavy nuclides (Jha and Dube, 1952) but it is of no help in all the cases $Z = 83$, 84, 85 in the medium heavy and heavy regions.

The failure of Fermi's formula may perhaps be attributed to the absence of a suitable correction-term similar to the one proposed by Stern for heavy elements.

Correction-term to Fermi's formula

Duckworth's recent mass spectrographic data (Duckworth, Preston, 1951; Duckworth, Strasford *et al.*, 1951) and their comparison with calculated masses from Fermi's formula [equation (2)] have made it possible to estimate the correction-term which is found to fit bettter with the observed values. The calculated masses from Fermi's formula have been compared with the observed data for $Z = 92$, 90, 82 and 78 in the table III. It is seen

TABLE III

Nuclides	Mass observed in a.m.u.	Mass calculated in a.m.u.	Difference	Mass calculated using correction-term
$_{92}U^{238}$	238·1241±10	238·1205	·0036	238·1218
U^{235}	235·1156±10	235·1130	·0026	235·1165
U^{234}	234·1129±10	234·1107	·0022	234·1139
$_{90}Th^{232}$	232·1093±10	232·1069	·0024	232·1085
$_{82}Pb^{208}$	208·0422±15	208·0591	−·0167	208·0436
Pb^{207}	207·0412±15	207·0576	−·0164	207·0439
Pb^{206}	206·0394±15	206·0550	−·0156	206·0425
$_{78}Pt^{196}$	196·0274±6	196·0379	−·0105	196·0244
Pt^{195}	195·0265	195·0366	−·0101	195·0245
Pt^{194}	194·0256±14	194·0341	−·0085	194·0232

that in some cases the calculated mass is higher than the observed one and in some cases lower, the difference Δm ranging from $+0{\cdot}004$ to $-0{\cdot}017$ mass units in the region $194 \leqslant A \leqslant 238$.

From the isotopes of U, Th, Pb, Pt, it is clear that Δm is a function of A and decreases with the decrease of A. But the dependence of correction-term on A only cannot be regarded as satisfactory. It depends on Z and increases with the decrease of Z. (It may be mentioned here that Stern's correction-term is independent of Z and increases with A like this correction-term.)

In the region of heavy nuclides, the experimental data are meagre. The atomic masses of Pt isotopes and of Pb^{208} are known accurately. The masses of Pb^{207} and P^{206} are determined from the known mass of Pb^{208} and the observed neutron binding energy in Pb^{208} and in $Pb.^{207}$

$$M(207, 82) = M(208, 82) - Mn + Bn(208, 82) \quad (4)$$

$$M(206, 82) = M(207, 82) - Mn + Bn(207, 82) \quad (4\,a)$$

where Mn = mass of the neutron = 1·00898 M.U. and the observed neutron binding energies in Pb^{208} and Pb^{207}, *i.e.*, Bn (208, 82) and Bn (207, 82) are 7·38 Mev. and 6·73 Mev. respectively (Harvey *et al.*, 1951, Kinsey *et al.*, 1950 and 1951).

It is difficult to get a simple correction-term which may satisfactorily represent the correction for all ranges of A. In the region of medium heavy and heavy nuclides correction

$$\Delta m = 0{\cdot}0290 - 3\,[KA^{1.2} - K'Z^{1.5}] \text{ in M.U.} \quad (5)$$

where

$$K = 0{\cdot}0002 \text{ and } K' = 0{\cdot}00014.$$

The masses calculated with this correction-term differ from the observed ones by values ranging from ·0003 to ·003 mass units in the medium heavy region.

Calculation of E_α using the correction-term

With the introduction of this correction-term in Fermi's formula, the calculated E_α is modified considerably. The correction to E_α in Mev. is given by

$$\Delta E_\alpha = K_1\,[Z^{1.5} - (Z-2)^{1.5}] - K_2\,[A^{1.2} - (A-4)^{1.2}] \text{ Mev.} \quad (6)$$

where

Where $K_1 = 0{\cdot}39108$ and $K_2 = 0{\cdot}55869$ for medium heavy and heavy nuclides. The calculated alpha-disintegration energy using this correction-term, *i.e.*, $E_\alpha + \Delta E_\alpha$ are given in the last columns of Tables I and II.

DISCUSSION OF RESULTS

There is a numerical agreement between the observed data and the calculated values using the correction-term in the region of heavy nuclides. In the region of 126 neutrons, there is some improvement, the difference between the observed and calculated values for At^{213}, Po^{212} and Bi^{211} is of the order of 4 Mev., 4·4 Mev. and 2·2 Mev. respectively which can satisfactorily be explained on the nuclear shell-structure.

The mass numbers of gold and mercury isotopes which are short-lived alpha-emitters have been tentatively assigned to lie between 185 and 188 and the alpha decay energies are 5·07 and 5·6 Mev. respectively. These results agree with the calculated ones for the isotopes having mass numbers 188.

REFERENCES

Barton, G. W., Ghiorso, J. A. and Perlman, I. — *Phys. Rev.*, 1951, **82**, 13.

Bethe-Weizsacker .. *Rev. Mod. Phys.*, 1936, **8**, 82.

Bohr and Wheeler .. *Phys. Rev.*, 1939, **56**, 426.

Das .. *Ind. J. Phys.*, 1950, **24**, 523.

Dempster, A. J. .. *Phys. Rev.*, 1948, **73**, 1125.

Duckworth, H. E. and Preston, R. S. *Ibid.*, 1951, **82**, 468.

———, Kegley, C. L., Olsan, J. M. and Strasford, G. S. *Ibid.*, 1951, **83**, 1114.

Harvey .. *Ibid.*, 1951, **81**, 353.

Jha, S. and Dube, G. P. .. *Ind. J. Phys.*, 1952, **26**, 15.

Kinsey .. *Phys. Rev.*, 1950, **78**, 77.

———— .. *Ibid.*, 1951, **8**, 388.

Kohman .. *Ibid.*, 1949, **76** 448.

Magnusson, L. B., Thompson, S. G. and Seaborg, G. T. *Ibid.*, 1950, **78**, 363, for data for alpha-emitters. *Nuclear Physics* by E. Fermi (Chicago University Press, 1951 edition, page 7.

Perlman, I., Ghiorso, A. and Seaborg, G. T. *Phys. Rev.*, 1950, **77**, 26.

——— and Seaborg, G. T. .. *Rev. Mod. Phys.*, 1948, **20**, 585, for data for alpha-emitters.

Precy .. *Proc. Phys. Soc.*, 1950, **63A**, 692.

Rasmussen *et al.* .. *Phys. Rev.*, 1950, **80**, 475.

Rasmussen, J. O., Thompsen, Jr. S. G. and Ghiorso, A. *Ibid.*, 1953, **89**, 33.

Saha and Saha .. *Trans. Nat. Inst. of Sci. Ind.*, 1949, **2**, 193.

Stern, O. .. *Rev. Mod. Phys.*, 1949, **21**, 316.

Thompson and Ghiorso *et al.* .. *Phys. Rev.*, 1949, **76**, 1406.

Weaver, Boyd .. *Ibid.*, 1950, **80**, 301.

KINETICS OF THE OLEFINE-BROMINE REACTION

Part VII. The Reaction between Cortonic and Dimethyl Acrylic Acids and Bromine in Carbon Tetrachloride*

By I. M. Mathai and S. V. Anantakrishnan, F.A.Sc.

(Department of Chemistry, Madras Christian College, Tambaram, S. India)

(Originally received January 19, 1954

Received in revised form May 27, 1954)

Studies of the reaction in glacial acetic acid have been reported in earlier parts.[3] It was then considered desirable to extend the observations to non-hydroxylic solvents and preferably nonpolar solvents. The results of experiments in carbon tetrachloride are reported here.

From the trend of observations in other solvents[2, 5, 7] that had been reported by different workers and from observations of the reaction in the gas phase,[6] it was anticipated that the reactions in this solvent will involve a polar surface. Now, all heterogeneous reactions involve the adsorption of one or more reactants in a single or a multimolecular layer and it is necessary also to note the influence of the nature of the surface on such adsorption. In the exploratory work, it is desirable to avoid other complications and in spite of the disadvantages of choosing carboxylic acids, these compounds have been taken up for study. This avoids the complication of the peroxide effect known to be negligible in these and also enables a comparison with the work in other solvents.

Experimental

(i) *Material used*

Carbon tetrachloride.—Pure carbon tetrachloride was kept in contact with an acid solution of potassium dichromate for three days with frequent shaking. The carbon tetrachloride was then separated, washed with distilled water, then with a dilute solution of potassium hydroxide and then again with distilled water. The moist solvent was then dried over anhydrous calcium chloride for several days and fractionated. The middle fraction, b.p. 76·6–76·8/760 mm., was collected and stored over sticks of potassium hydroxide in amber coloured bottles. The use of phosphorous pentoxide for drying this solvent was found to be unsatisfactory and gave erratic results for the course of this reaction. A report of the dielectric constant studies on this apsect of the work is being published separately.

* Based on the thesis of I.M.M. accepted for the M.Sc. degree of Madras University.

Trans-Crotonic acid.—The product supplied by Tennessee Eastman Corporation was used after purification by repeated fractional crystallisation from petroleum ether (60–80°) to constant m.p. and stored in the dark, over anhydrous calcium chloride in a vacuum desiccator. The choice of this procedure was necessitated by the need for minimising the chances of conversion to the *cis* form. Freshly recrystallised samples, m.p. 72° C., was used for each experiment.

2 : 2 *Dimethyl acrylic acid.*—The compound was prepared essentially by the method of Barbier and Glaser.[4] Mesityl oxide (1 mole) was oxidised by an alkaline hypochlorite solution (2 moles hypochlorite and 4 moles sodium

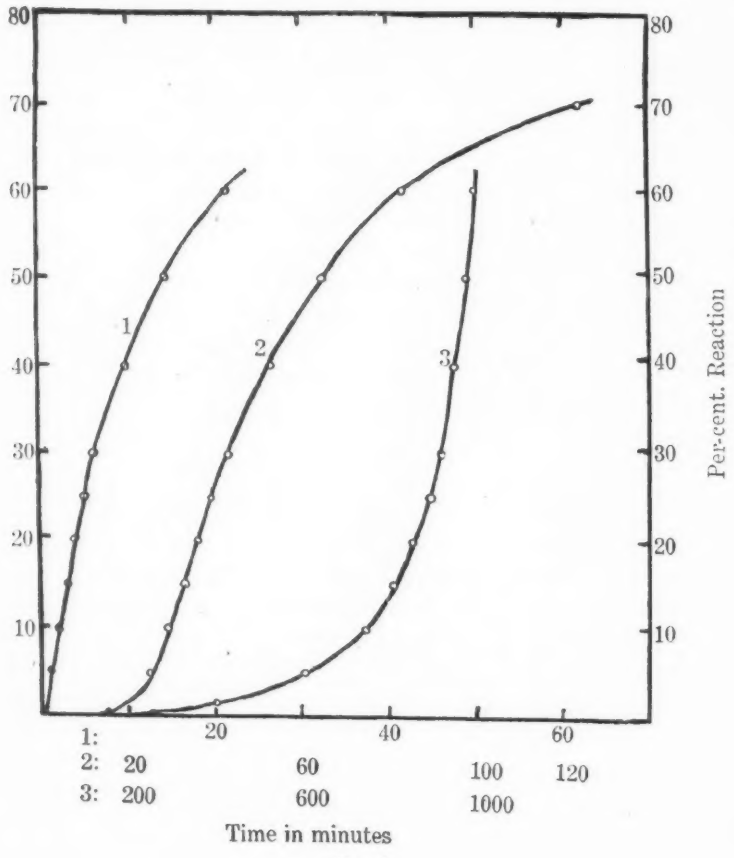

FIG. 1

Reaction between dimethyl acrylic acid and bromine at different concentrations.

hydroxide) keeping temperatures below — 5° C. Excess hypochlorite was destroyed by bisulphite and after the removal of the byproduct, chloroform, the solution was acidified with dilute sulphuric acid, keeping temperatures low. Dimethyl acrylic acid separated on standing and a further yield was obtained by ether extraction of solution (yield 70% of theory). The acid was recrystallised from hot water and stored in a desiccator in the dark over phosphorous pentoxide, m.p. 70° C.

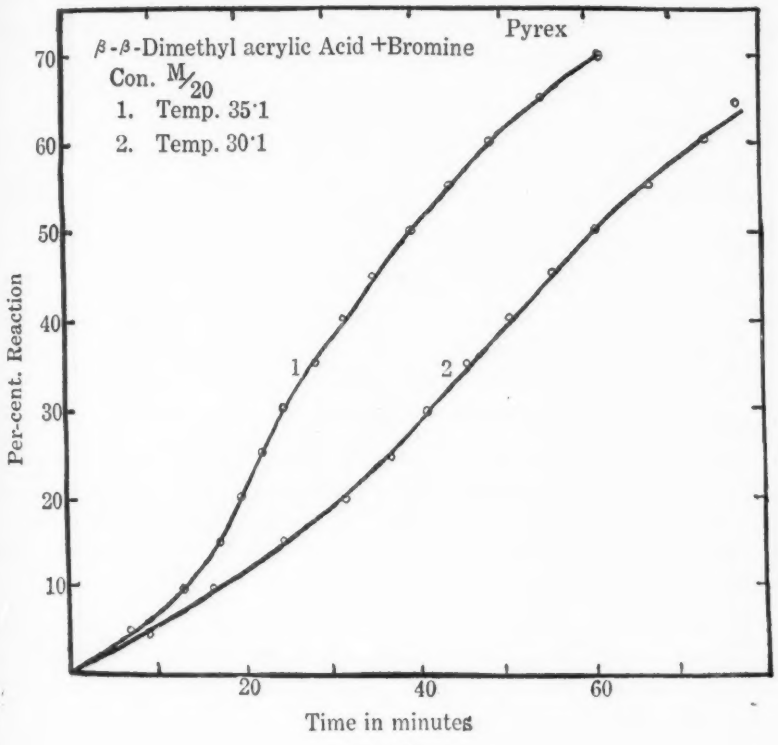

FIG. 2

Bromine was prepared by the method indicated by one of us earlier and the purity checked from time to time.[1]

(ii) *Materials added for increasing surface*

Sodium bromide, barium sulphate and lithium bromide, of analytical reagent quality, were dried at 120° C. and stored in a desiccator before use. Alumina, silica and pyrex glass beads were used to provide additional surface.

The beads were treated by the same procedure, with reagents used at the same concentration and in the same order and prepared fresh for each experiment. The beads were soaked in a chromic acid solution for about 12 hours, with frequent shaking, washed thoroughly with distilled water, refluxed thrice with distilled water for 10 minutes at a time and then dried in an air oven at 120° C. for three hours. The beads used were uniform in each case, the pyrex beads being spherical and the others cylindrical. As a first approximation, the surface area was calculated for these shapes from the dimensions and in the different runs, the surfaces were assumed to be proportional to the weights. The relevant data for the purpose are given in Table I.

TABLE I

Material of bead	Average radius		l	Average surface sq. cm.	No. of beads for 100 g.
	External	Internal			
Pyrex ..	..	0·287 cm.	..	1·035	377
Silica ..	0·260	0·125	0·675	1·959	456
Alumina ..	0·293	0·157	0·638	2·188	260

(iii) *Reaction Vessels and Measuring Vessels*

250 ml. and 100 ml. amber coloured Pyrex bottles with well ground stoppers were used as the reaction vessels. The bottles were kept with chromic acid for 24 hours, washed thoroughly with distilled water and then steamed. The vessels were then dried in an air oven at 120° C. for about four hours and kept overnight in a vacuum desiccator.

All measuring vessels were standardised and coated with black enamel and were submitted to the same treatment as the reaction vessels and were used only after 24 hours at room temperature. Under these conditions volume changes were found to be negligible.

The reactions were carried out in an electrically maintained thermostat (temperature controlled to within 0·005° C.). All vessels were tested for evaporation losses, using bromine solutions. The course of the reaction was followed by the iodometric estimation of the unreacted bromine, in aliquot parts, from time to time. Rapid estimations were necessary as some of the dibromides formed slowly liberate iodine.

To economise space, only a few typical runs are presented in the accompanying tables and figures.[1]

TABLE I

Reaction between Bromine and Trans-Crotonic Acid at 35·1° C.

Concentration of olefine / Concentration of bromine	0·2000 M / 0·2093 M A		0·1000 M / 0·1004 M B		0·0500 M / 0·0503 M C		0·0500 M / 0·05055 M D		0·0500 M / 0·0503 M E	
A Time (min.) ..	0	2·25	7·25	14·5	25·5	45	83·25	350	1086	2300
Titre ..	19·60	19·60	19·50	19·20	18·80	18·20	17·80	16·25	13·90	11·50
% Br reacted	0	0	0·51	2·04	4·08	7·15	9·18	17·09	29·08	41·32
B Time (min.) ..	0	38·0	94·11	199·4	783	2705	5465	8102		
Titre ..	9·40	9·40	9·10	9·00	8·50	7·40	6·35	5·40		
% reaction ..	0	0	3·19	4·26	9·57	21·27	33·21	42·56		
C Time (min.) ..	0	8·05	215·5	744	1114	2749	5265	6768		
Titre ..	9·20	9·20	9·10	8·80	8·55	7·70	6·55	5·95		
% reaction ..	0	0	1·09	4·35	7·07	16·30	29·47	34·25		
D Time (min.) ..	0	106·8	227·1	683	1060	2494	3221	3983	Pyrex Bead	
Titre ..	9·30	9·00	8·70	7·95	7·40	5·45	4·90	4·50	Surface	
% reaction ..	0	3·23	6·45	14·32	20·43	41·40	47·32	51·60	585·2 sq. cm.	
E Time (min.) ..	0	136·25	312	1051	1780	2517·5	3832	5991	Silica bead	
Titre ..	9·20	9·00	8·85	7·85	7·00	6·40	5·35	4·00		
% reaction ..	0	2·17	3·80	14·68	23·91	30·45	41·85	53·26		

TABLE II

Reaction between Bromine and 2-2 Dimethyl Acrylic Acid at 35·1° C.

Concentration of olefine / Concentration of bromine	0·1000 M / 0·1009 M A		0·0500 M / 0·04956 M B		0·0250 M / 0·02532 M C		
A Time (min.) ..	0	1·08	3·62	6·17	12·33	16·70	23·40
Titre (ml.) ..	19·50	18·00	16·20	13·75	10·80	9·15	7·10
% Bromine reacted ..	0	7·69	16·42	29·49	44·62	53·08	63·08
B Time (min.) ..	0	11·70	21·43	29·07	36·53	42·74	61·50
Titre ..	9·35	9·35	9·15	8·40	7·40	6·45	4·90
% Bromine reacted ..	0	0	2·14	10·16	20·85	31·01	47·62
C Time (min.) ..	0	328	687	775	850	942	985	999
Titre (ml.) ..	10·00	9·70	9·30	8·85	8·20	6·40	4·95	4·00
% Bromine reacted ..	0	3·0	7·0	11·5	18·0	36·0	50·5	60·0

TABLE III

Influence of Surface on the Reaction between Bromine and Olefine for an Olefine Concentration of 0·0500 M at 30·1° C.

Bromine Concentrations: same order but slightly different.
A: Typical runs with added pyrex beads; B: Typical runs with silica beads.

A	Crotonic acid	Time ..	0	106–8	272	683	1060	2494	3983
		Titre ..	9·30	9·00	8·70	7·95	7·40	5·45	4·50
		% reaction ..	0	3·23	6·45	14·32	20·43	41·40	51·60
	2–2 Dymethyl acylic acid	Time ..	0	6·70	19·50	31·37	45·78	60·80	82·32
		Titre ..	10·40	10·00	9·10	8·40	6·80	5·20	3·70
		% reaction ..	0	3·85	12·50	19·23	34·61	50·00	64·43
B	Crotonic acid	Time ..	0	136	1051	1780	2959	5991	
		Titre ..	9·20	9·00	7·85	7·00	5·80	4·00	
		% reaction ..	0	2·17	14·68	23·91	36·96	53·26	
	2–2 Dimethyl acrylic acid	Time ..	0	12·22	23·87	29·97	39·52	46·95	74·77
		Titre ..	10·55	9·85	8·90	8·20	7·25	6·40	4·40
		% reaction ..	0	6·63	15·64	22·47	31·27	39·42	58·29

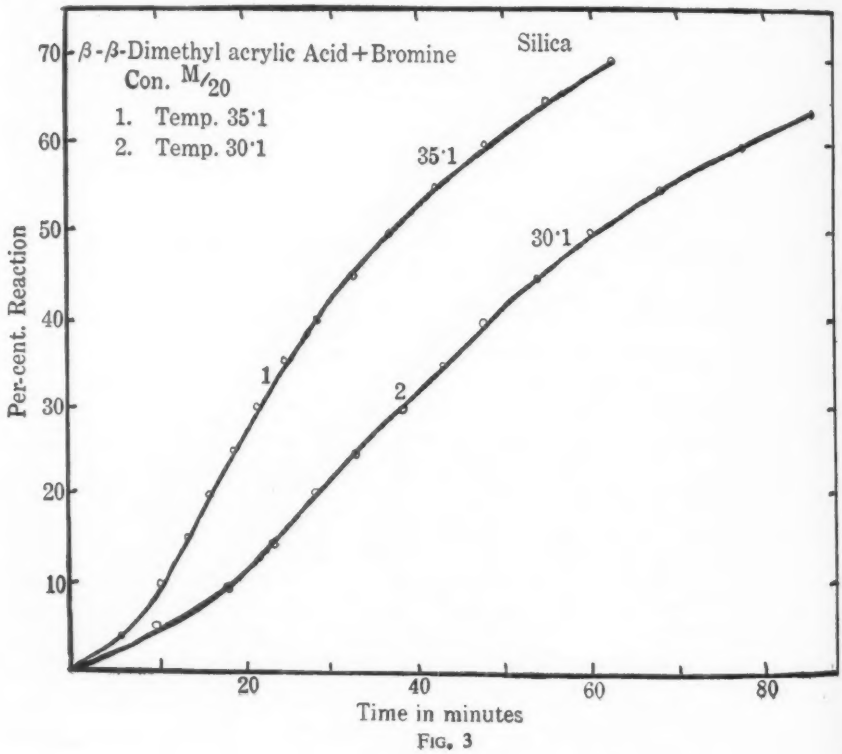

FIG. 3

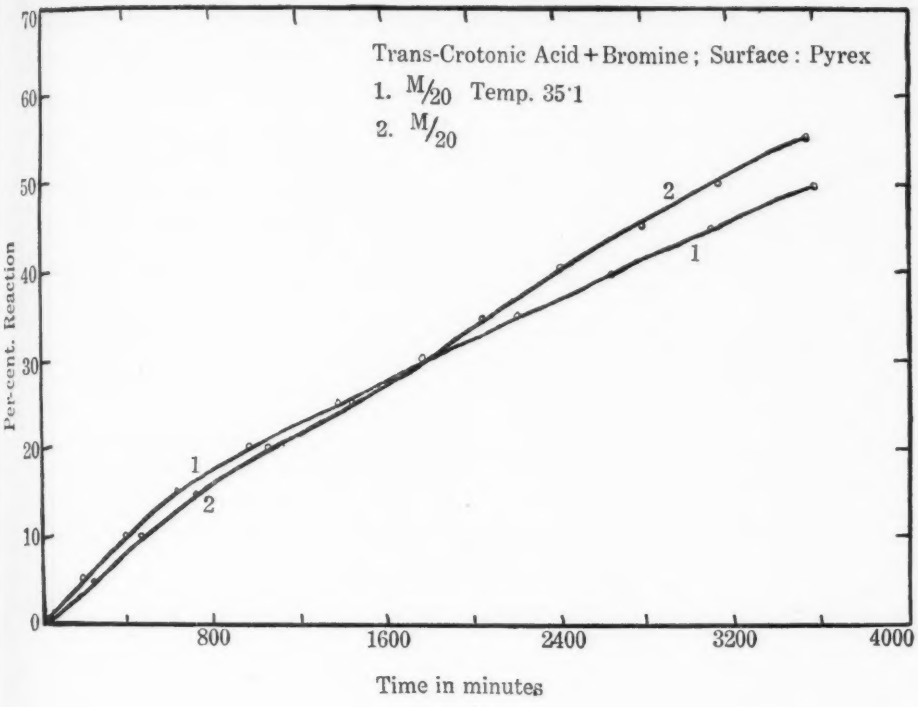

FIG. 4

DISCUSSION OF RESULTS

Schwab[9] has remarked that where there is a surface reaction between ethylene and the halogens, both reactants are slightly adsorbed and the experiments of Gwyn Williams[6] have borne out these. The typical runs are reported below and the illustrative curves (Figs. 2, 3 and 4) show the trend.

An inspection of these shows clearly the presence of an induction period which is sensitive to changes in the concentration of reactants as well as changes in the structure of the olefine and in the case of crotonic acid the reaction even appears to have a negative temperature coefficient. It is generally considered that reactions in carbon tetrachloride simulate a gas reaction. Preliminary experiments have shown that both reactants are adsorbed in varying amounts. A fuller study of this is in progress. The heterogeneous reaction is unmistakably shown by the elimination of the induction period and a quickening of the reaction by packing the vessel with beads of different materials.

A qualitative comparison shows that the effectiveness of the surface in catalysing the reaction is in the order

Pyrex glass > Silica (fused) > Alumina (fused)

A rough comparison can be made by transforming the results obtained so that they refer to the same surface area. As a first approximation, one may assume that the time required for a given fraction of the reaction is inversely proportional to the surface. The results obtained by such computation are given in Tables IV and V below.

TABLE IV

Reaction between Dimethyl Acrylic Acid and Bromine: at Constant Surface Area

Concentration	Surface	Time for 25% reaction min.		Time for 50% reaction min.	
		30° C.	35° C.	30° C.	35° C.
0·066 M	Pyrex ..	16·1		40·0	
	Silica ..	30·8		80·9	
	Alumina ..	39·4		86·7	
0·05 M	Pyrex ..	42·6	17·3	70·8	30·4
	Silica ..	53·9	25·3	111·2	48·5
0·025 M	Pyrex ..		139·0		216·0
	Silica ..		197·0		283·0

Note: There have been small variations in the bromine concentrations.

TABLE V

Reaction between Trans-Crotonic Acid and Bromine at Constant Surface Area at 35° C.

Concentration	Surface	Time for 10% reaction min.	Time for 25% reaction min.	Time for 50% reaction min.
0·1 M	Pyrex ..	450	1103	4622
	Silica ..	665	3036	
0·05 M	Pyrex ..	535	1172	4207
	Silica ..	945	1984	6823

An inspection of the tables clearly shows pronounced differences between the two acids. While consideration of structural factors may be deferred, the first stage in any mechanistic study is an analysis of the reaction order and the trend of rate constants. In spite of the choice of a nonpolar solvent, a heterogeneous reaction in solution may not show the simplicity of a gas reaction. The present observations are also inadequate for assessing the influence of the products of the reaction. It is also likely that there is a simultaneous homogeneous reaction.

Taking the time required for a given fraction of a reaction, the figures obtained lead to an approximate relationship

$$(c_1/c_2)^3 = t_2/t_1$$

in the initial stages, but, the right-hand side tends to smaller values as the reaction proceeds, the equality being nearly reached when the square of the concentration terms are used. With silica surfaces, the third power relationship does not hold even at the start and falls off later to the first power.

In acetic acid solutions, Robertson and co-workers[8] find that the reaction is of the third order at the low temperatures at which they worked while Anantakrishnan and Venkatarman working at or above 30° C. find that the reaction is of the second order. The gas reaction according to Gwyn Williams[6] is apparently of the third order. The difficulty in accepting a third or higher order for the reaction is the definite positive temperature coefficient, though the position is rather complex with crotonic acid which has a small negative temperature coefficient.

It is quite clear, however, that the reaction requires a polar environment for initiation of the reaction, though, it is just possible, that the polarised molecule after leaving the surface may initiate the homogeneous phase of the reaction in the nonpolar solvent also. The data so far obtained is not adequate for the purpose of separating the two phases of the reaction. Preliminary experiments have shown that the addition of dry crystals of sodium bromide or barium sulphate accelerate the reaction while the relative influences of the three different surfaces studied indicate that the presence of both cations and anions at the surface facilitate the reaction. Using only glassy surfaces, it is not practicable to study the geometrical factor but complex silicates appear to afford a better environment than either silica or alumina.

We have to thank the Tennessee Eastman Corporation for a gift of the crotonic acid used.

SUMMARY

The reaction between trans-crotonic acid as well as 2: 2-dimethyl acrylic acid and bromine has been studied in carbon tetrachloride solution in the dark. The reaction is found to be quite a complex one involving both homogeneous and heterogeneous phases. The course of the reaction is governed by the nature of the olefine and the nature of the catalysing surface.

REFERENCES

1. Anantakrishnan, S. V. .. *J. Annamalai Univ.*, 1942, **11**, 170.
2. ——— and Ingold, C. K. .. *J.C.S.*, 1935, 984.
3. ——— and Venkataraman, R. .. *Proc. Ind. Acad. Sci.*, 1946, **23A**, 306.
4. Barbiere and Glaser .. *Bull. Soc. Chim.*, 1905, **33**, 185.
5. Bauer and Daniels .. *J.A.C.S.*, 1934, **56**, 378, 2014.
6. Gwyn and Williams .. *Trans. Farad. Soc.*, 1942, **37**, 749.
7. Plotnikow .. *Z. Physik. Chem.*, 1905, **53**, 605.
8. Robertson, P. W., *et al.* .. *J.C.S.*, 1945, 130, etc.
9. Schwab, G. M. .. *Die catalyse*, 1931.

1040-54 Printed at The Bangalore Press, Bangalore City, by C. Vasudeva Rao, Superintendent and Published by The Indian Academy of Sciences, Bangalore

NOTICE TO AUTHORS

Scientific papers intended for publication in the *Proceedings of the Indian Academy of Sciences* can be accepted only when they are communicated by a Fellow of the Academy whose duty shall be to satisfy himself that such communications are fit to be read at the Meeting of the Academy and published in its *Proceedings*.

Papers should not ordinarily exceed fifty pages of foolscap. MSS. should be either typewritten or written in legible hand on one side of the paper. All papers should be carefully revised by the authors and should be absolutely in final form for printing. Position for text-figures should be indicated. Each paper shall conclude with a critical summary not exceeding 350 words.

Drawings, diagrams or other illustrations should be made on larger scale (preferably) twice the size than the ones in which they are intended to appear. They should be done in Indian ink on bristol board with lettering in pencil. Scale of magnification of camera lucida tracings should be indicated by the side of drawings. In certain special cases arrangements will also be made for monochrome lithographic and other colour plates. Reduction of illustrations desired should be indicated in pencil. Appropriate legends should accompany all drawings. Names of authors are to be marked in pencil on the left-hand corner of drawing sheets. Photomicrographs should be securely mounted with colourless paste.

All tables, quotations and footnotes which will be set hereafter (beginning from Vol. I, No. 2) in types smaller than the text, should be typewritten on separate sheets and placed with the text in proper sequence. Footnotes should be numbered in Arabic numerals.

References to literature in the text should be given, whenever possible, in chronological order, only the names of authors and years of publication, in brackets, being given. They should be cited in full after the summary, the authors' names following in alphabetical order. Thus,

Name or Names of author; Name of Journal (abbreviation) with a single underline; Year of publication; Number of Volume with a double underline, and lastly page. The following would be a useful illustration:—

Bergmann and Stather . . . . . Z. Physiol. Chem., 1926, 152, 189.

Two copies of slip-proof and wherever possible, a page proof for final revision will be sent to authors. All corrections are best made on the slip-proof which should be transmitted to the Office of the Academy. All proof corrections involve heavy expenses which would be negligible if the papers are carefully revised by the authors before submission.

Authors will be supplied with reprints of their papers at cost price, if intimation is given at the time of returning the slip-proof.

Blocks appearing in the *Proceedings* will be available for purchase by their respective authors. Orders for the same should be sent along with the corrected proofs and in any case not later than one month after the date of publication of the paper. The price charged would be 25% of the actual cost of the blocks *plus* freight and despatching charges. If the blocks are reproduced in other journals or publications, due acknowledgment should be made in them to the *Proceedings*.

The original drawings and plates of blocks appearing in the *Proceedings* will be returned to such of the authors as may require them provided the cost of despatching such originals is borne by them.

CONTENTS

PAGE

The Structure and Optical Behaviour of Iridescent Calcite . . . . . Sir C. V. Raman and A. K. Ramdas 1

On the Distribution of Thermal Neutrons from a Fast Neutron Source Placed at the Interface of Two Media . R. Ramanna and S. B. D. Iyengar 8

Heterocyclic Compounds. Part II. Synthesis of 4-Quinazolones with Substituents in the 2- and 3-positions . . . . . M. R. Subbaram 22

Generalized Singular Points with Applications to Flow Problems . . . . . B. R. Seth 25

On the Semi-Empirical Mass-Formula and Alpha-Disintegration Energy in the Region of Heavy and Medium Heavy Nuclides . . . . . G. P. Dube and Lal Saheb Singh 37

Kinetics of the Olefine-Bromine Reaction. Part VII. The Reaction between Cortonic and Dimethyl Acrylic Acids and Bromine in Carbon Tetrachloride . . . . . I. M. Mathai and S. V. Anantakrishnan 47